

Structure–Activity Relationship Study of Betulinic Acid, A Novel and Selective TGR5 Agonist, and Its Synthetic Derivatives: Potential Impact in Diabetes[¶]

Cédric Genet,^{†,‡} Axelle Strehle,[§] Céline Schmidt,^{||} Geoffrey Boudjela,[⊥] Annelise Lobstein,[○] Kristina Schoonjans,[#] Michel Souchet,[⊥] Johan Auwerx,[#] Régis Saladin,^{*,||} and Alain Wagner[†]

[†]UMR/CNRS 7199, Faculté de pharmacie, Université Louis Pasteur, 67404 Illkirch, France, ^{*}Novalix, Bioparc, Boulevard Sébastien Brant, BP30170, 67405 Illkirch, France, [§]Institut de Génétique et de Biologie Moléculaire et Cellulaire, CNRS/INSERM/université Louis Pasteur, 67404 Illkirch, France, ^{||}PhytoDia, Bioparc, Boulevard Sébastien Brant, BP10413, 67404 Illkirch, France, [⊥]Harmonic Pharma, Espace Transfert, 615 rue du Jardin Botanique, 54600 Villers les Nancy, France, [○]UMR/CNRS 7175, Faculté de pharmacie, Université Louis Pasteur, 67404 Illkirch, France, and [#]Swiss Federal Institute of Technology, CH-1015 Lausanne, Switzerland. [¶]Crystal structure deposit number: The crystal structure of **18 dia 1** has been deposited at the Cambridge Crystallographic Data Center and the allocated deposition number is CCDC 741328.

Received June 15, 2009

We describe here the biological screening of a collection of natural occurring triterpenoids against the G protein-coupled receptor TGR5, known to be activated by bile acids and which mediates some important cell functions. This work revealed that betulinic (**1**), oleanolic (**2**), and ursolic acid (**3**) exhibited TGR5 agonist activity in a selective manner compared to bile acids, which also activated FXR, the nuclear bile acid receptor. The most potent natural triterpenoid betulinic acid was chosen as a reference compound for an SAR study. Hemisyntheses were performed on the betulinic acid scaffold, and we focused on structural modifications of the C-3 alcohol, the C-17 carboxylic acid, and the C-20 alkene. In particular, structural variations around the C-3 position gave rise to major improvements of potency exemplified with derivatives **18 dia 2** (RG-239) and **19 dia 2**. The best derivative was tested *in vitro* and *in vivo*, and its biological profile is discussed.

Introduction

Diabetes is a major worldwide health problem. In 2000, 171 million people were living with diabetes, and this number is projected to rise to 366 million in 2030.¹ The huge human and economic costs of diabetes and associated complications prompted the research for appropriate and efficient treatments. All current therapies target only the consequences of diabetes, and it could therefore be of particular interest to identify compounds that act in the early stages of diabetes. Obesity and insulin resistance, which generally precede type 2 diabetes, are correlated with mitochondrial dysfunction in skeletal muscle.² Identification of new biological targets, which interfere with mitochondrial function, could therefore be relevant to prevent and treat type 2 diabetes.

In addition to their well-established roles in dietary lipid absorption and cholesterol metabolism, bile acids (BAs) have been shown to activate mitogen-activated protein³ and nuclear hormone receptors such as farnesoid X receptor α (FXR- α).⁴ Through activation of these two pathways, BAs can regulate their own metabolism. BAs are also ligands for the

G-protein coupled receptor TGR5,⁵ and activation of this receptor by bile acids results in an effect on energy homeostasis. Indeed, the administration of BAs to mice fed with a high fat diet increases energy expenditure in brown adipose tissue, preventing obesity and insulin resistance.⁶ The processes involved implicate TGR5 activation by BAs which results in an increase in cAMP production in brown adipose tissue. Subsequently, the function of the thyroid hormone activating enzyme deiodinase type 2 is improved, leading to an increase in mitochondrial function and thus energy expenditure.⁶ Consistent with the role of TGR5 in the control of energy metabolism, female TGR5 knockout mice show a significant fat accumulation with body weight gain when challenged with a high fat diet, indicating that the lack of TGR5 receptor decreases energy expenditure and promotes obesity.⁷ In addition and in line with the involvement of TGR5 in energy homeostasis, BA activation of the membrane receptor has also been reported to promote the production of glucagon-like peptide 1 (GLP-1) in murine enteroendocrine cell lines.⁸ All together, these data suggest that TGR5 is a relevant target to treat metabolic diseases.

Recently, and in contrast to BAs, which activate both TGR5 and FXR, a number of novel and selective TGR5 agonists that do not activate FXR have been described. A biological screening of a collection of natural occurring bile acids, bile acid derivatives, and some steroid hormones has resulted in the discovery of new potent and selective TGR5 ligands such as 6 α -ethyl-23(*S*)methyl-chenodeoxycholic acid and derivatives.⁹ Furthermore, this study indicated that the binding pocket of TGR5 is endowed with a narrow hydrogen bonding door site recognizing the 3-hydroxyl group of BAs,

*To whom correspondence should be addressed. Fax: +33368854804. PhytoDia, Bioparc, Boulevard Sébastien Brant, BP10413, 67412 Illkirch, France. E-mail: rs@phytodia.com.

^a Abbreviations: FXR, farnesoid X receptor; Bas, bile acids; DMAP, dimethylamino pyridine; NaH, sodium hydride; MeI, methyl iodide; Pd/C, palladium on carbon; Cs₂CO₃, cesium carbonate; BnCl, benzyl chloride; EDC, 1-ethyl-3-(3-dimethylaminopropyl) carbodiimide; HOBt, hydroxybenzotriazole; NEt₃, triethylamine; TsCl, tosyl chloride; TMSCHN₂, trimethylsilyldiazomethane; DPPA, diphenylphosphine azide; mCPBA, meta-chloroperoxybenzoic acid; BH₃, boron hydride; LCA, lithocholic acid; CrO₃, chromium trioxide; C₆H₆, benzene; p-TSA, *p*-toluenesulfonic acid; NH₂OH.HCl, hydroxylamine hydrochloride; TsCl, tosylchloride.

a hydrophobic pocket lining to the C₆ and C₇ position of BAs, and a large and neutrally formal charged pocket that anchors the acidic side chain. That information was instrumental to design novel selective and potent BAs as TGR5 agonists.

In parallel, we demonstrated that oleanolic acid (**2**), a triterpenoid extracted from *Olea europaea* leaves, is a highly selective and potent TGR5 agonist and possesses an antihyperglycaemic effect.¹⁰ Encouraged by these results, we decided to investigate if other members of the triterpenoid family would also have TGR5 activity. To this end we have thus performed a biological screening of the natural occurring triterpenoid library. Among this triterpenoid library, betulinic acid (**1**) was chosen as lead compound for our structure–activity relationship (SAR) because of its higher TGR5 potency. A collection of betulinic acid derivatives was completed by hemisyntheses and provided more potent TGR5 agonists, illustrated by **18 dia 2** (RG-239). Then, the biological effect of the most efficient derivative, **18 dia 2**, made from nucleophilic attack of an allylic organomagnesium on the C-3 ketone was evaluated *in vitro* and *in vivo*. Finally, a ligand-based modeling study was performed to improve our understanding toward the TGR5 binding requirement and to provide useful evidence for the design of the next TGR5 agonist generation.

Results

A set of natural triterpenoid molecules was first tested for its TGR5 agonist activity. As shown in Table 1, betulinic acid (**1**), with an EC₅₀ = 1.04 μM and an efficacy of 83%, had better activity and efficacy compared to the other tested triterpenoids such as the initial active principle identified **2** (EC₅₀ = 2.25 μM, eff. = 72%) and the other active natural triterpenoid, ursolic acid (**3**) (EC₅₀ = 2.25 μM, eff. = 72%). Moreover, **1** appeared to be readily available by extraction or from commercially available sources, which is the main reason why it was chosen as a starting material in hemisyntheses for this SAR study.

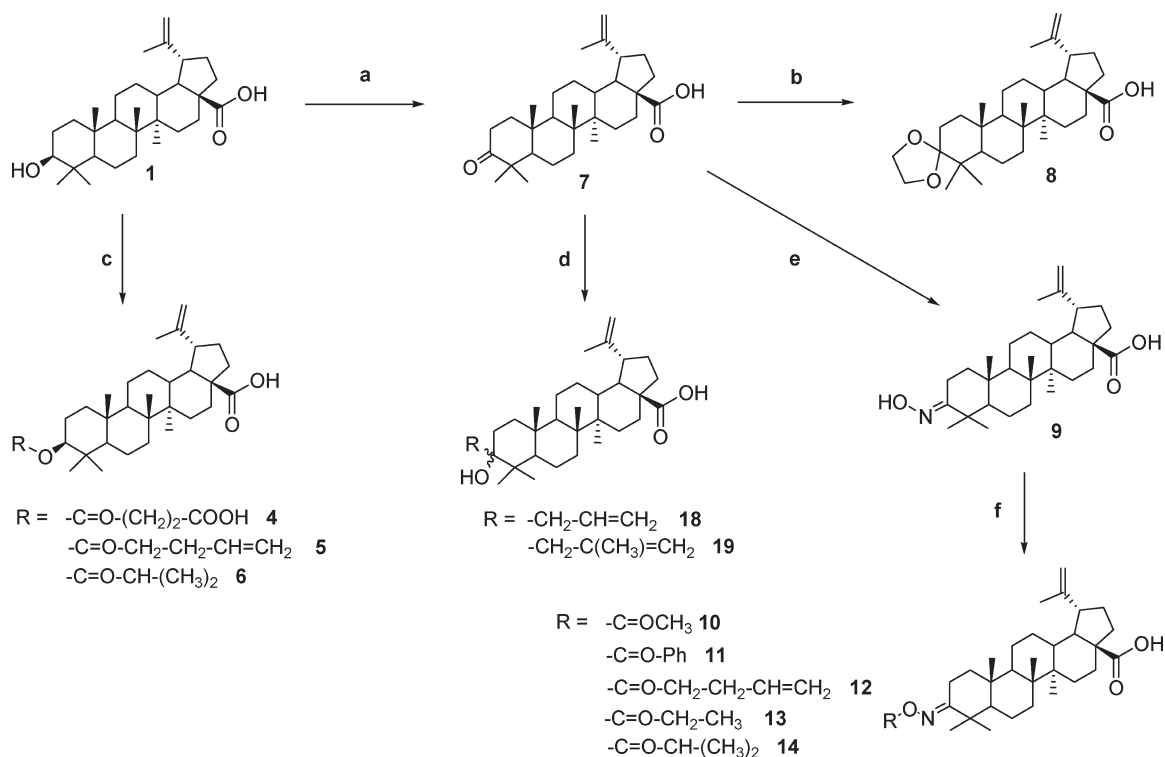
To investigate the binding at the two key positions C-3 and C-17, our work was first focused on (i) the modification of chemotypes like the hydroxyl group into ester, ketone, oxime, and on the stereochemistry of isomers at C-3 (Schemes 1 and 2) and (ii) the conversion of the carboxylic acid into ester, amide, and urea (Schemes 3, 4, 5). Further investigations concerned modifications of the alkene group into ketone, alkane, epoxide, and alcohol (Scheme 6).

Modifications on the Hydroxyl Group at Position C-3 (Schemes 1 and 2). The betulinic acid C-3 alcohol was esterified by refluxing **1** with anhydride succinic, isobutyric, and 4-pentenoic with dimethylamino pyridine (DMAP) in pyridine to obtain derivatives **4**, **5**, and **6** (Scheme 1).¹¹

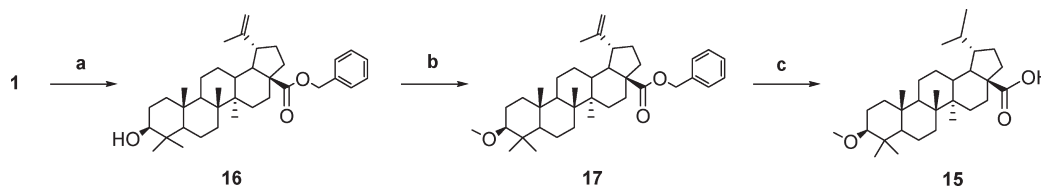
Then synthesis of ketone (**7**) was realized by oxidation of **1** using Dess Martin's reagent in DCM.¹² Derivative **7** was further modified into a hydrophobic acetal **8**.¹³ By heating under reflux ketone **7** in pyridine with hydroxylamine hydrochloride we obtained oxime **9** (Scheme 1).¹⁴ The syntheses of **10**, **11**, **12**, **13**, and **14** were obtained by refluxing **9** with DMAP and the corresponding anhydride in pyridine (Scheme 1).¹⁵ The monomethylated product **15** was synthesized in two steps. The benzylated protecting acid **16** in presence of sodium hydride (NaH) and methyl iodide (MeI) in DMF gave **17**¹⁶ which was finally hydrolyzed with a palladium on carbon catalyst (Pd/C) under H₂ (Scheme 2).^{17,18}

Table 1. TGR5 Activity of Natural Triterpenoids

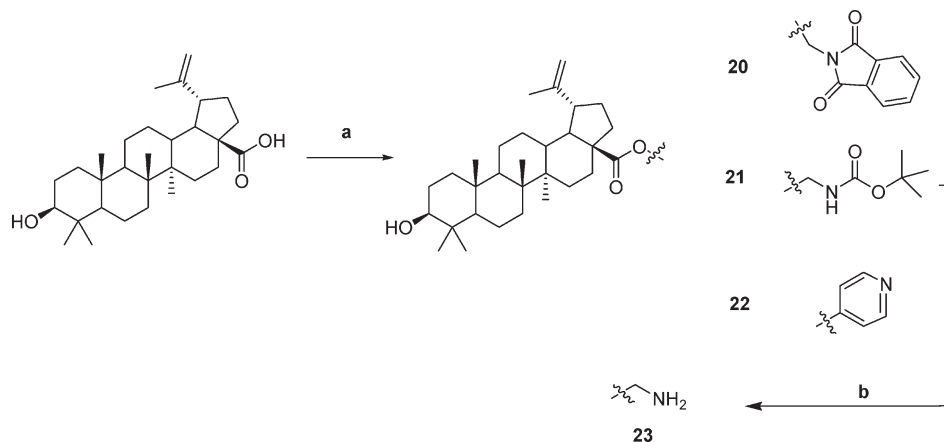
Name	structure	TGR5		FXR
		EC ₅₀ μM	Efficacy	EC ₅₀ μM
LCA litcholic acid		5.60	100	6.7
1 betulinic acid		1.04	83	0
2 oleanolic acid		2.25	72	0
3 ursolic acid		1.43	65	0
lupenone		>10	0	0
friedeline		>10	0	0
betulin		>10	0	0
uvaol		>10	0	0
α-amyrin		>10	0	0
arjunolic acid		>10	0	0
asiatic acid		>10	7	0
β-glycyrrhetic acid		>10	0	0
β-elemonic acid		>10	0	0

Scheme 1^a

^a Reagents: (a) Dess Martin's reagent, DCM, 4 h; (b) ethylene glycol, p-TSA, benzene, 15 h; (c and f) DMAP, anhydride, pyridine, reflux, 12 h; (d) RMgCl, THF, -78°C , 2 h; (e) $\text{NH}_2\text{OH}\cdot\text{HCl}$, pyridine, reflux 4 h.

Scheme 2^a

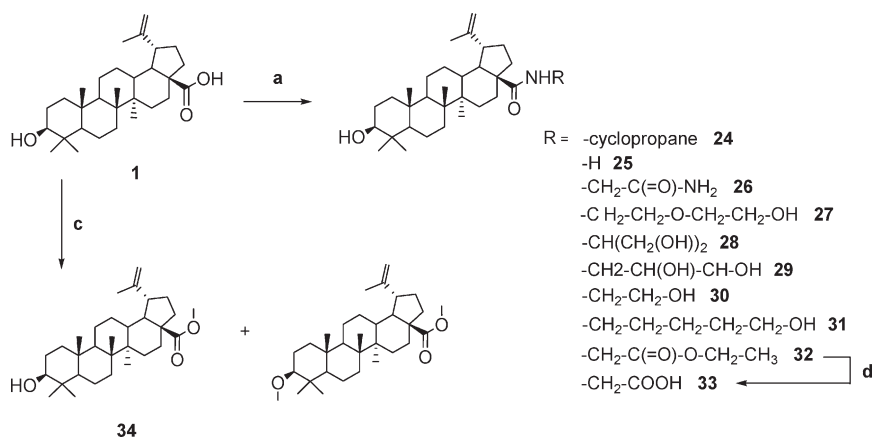
^a Reagents: (a) Cs_2CO_3 , BnCl, DMF, 5 h; (b) NaH, DMF, 2 h, MeI, 24 h; (c) Pd/C, H_2 , MeOH/THF, 12 h.

Scheme 3^a

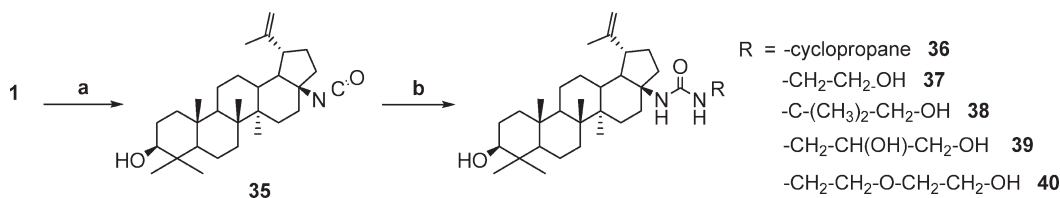
^a Reagents: (a) Cs_2CO_3 , DMF, 12–20 h; (b) MeOH, 4 M HCl/dioxane, 4 h.

The next step of our hemisynthesis exploration consisted of remodelling the C-3 chiral environment without neglecting to retain the free hydroxyl group. Ketone **7** was functionalized by a Grignard reaction to obtain new structures

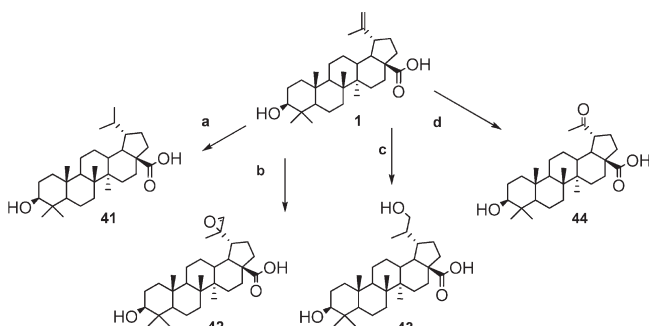
around the C-3 center.¹⁶ When adding an alkyl Grignard to **7** a rapid precipitation of a white solid corresponding to the magnesium carboxylate precluded the nucleophilic addition of the second equivalent of the alkyl Grignard to the

Scheme 4^a

^a Reagents: (a) EDC, HOBt, NEt₃, amine, DMF, 12–20 h; (b) TsCl, pyridine, DCM, 6 h; (c) TMSCHN₂, benzene, 2 h; (d) NaOH 4N, THF/EtOH, 14 h.

Scheme 5^a

^a Reagents: (a) DPPA, NEt₃, toluene, reflux, 19 h; (b) amine, toluene, reflux, 15 h.

Scheme 6^a

^a Reagents: (a) Pd/C, H₂, MeOH/THF, 24 h; (b) O₃, MeOH/CHCl₃, (Me)₂S, 30 min; (c) BH₃, THF, 0 °C 1 h, 16 h; (d) mCPBA, THF, 16 h.

ketone function. To circumvent this precipitation, the Grignard reagent had to be added slowly into a dilute solution. Treatment of the crude mixture with a dilute solution of HCl gave a mixture of two diastereoisomers in a 1/2 ratio (**dia 1**/**dia 2**) easily separated by silica gel column chromatography to afford **18 dia 1** and **dia 2** or **19 dia 1** and **dia 2**. The absolute configuration assignment of the C-3 chiral center was determined as “S” for **18 dia 1** by X-ray structure analysis (Figure 1). Other configurations were deduced from this result.

Modifications on the Carboxylic Acid Group at Position C-17 (Schemes 3 and 4). The chemical reaction between **1** and cesium carbonate (Cs₂CO₃) in DMF with the corresponding alkyl halide gave **20**, **21**, or **22** as esterification products (Scheme 3).¹⁹ Next, the amino group of **21** was deprotected in MeOH with 4 M HCl/dioxane to obtain free aliphatic amine **23** (Scheme 3).¹⁸

The carboxylic acid function was also converted into amide **24–32** by a peptide coupling reaction using 1-ethyl-

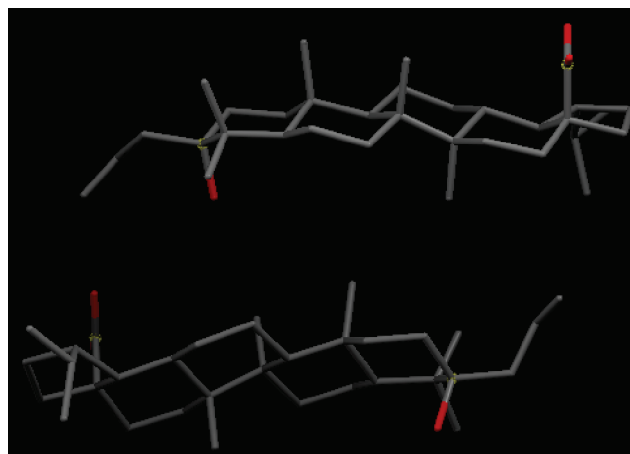


Figure 1. X-ray crystal structure of **18 dia 1**.

3-(3-dimethylaminopropyl) carbodiimide (EDC) and hydroxybenzotriazole (HOBt) as reagents (Scheme 4).²⁰

After formation of the ethyl amide **32**, its terminal ester group was hydrolyzed with 4 N NaOH in a mixture of THF/EtOH to acquire compound **27**.²⁰ Derivative **34** was isolated from a mixture of mono- and dimethylated products after the use of trimethylsilyldiazomethane (TMSCHN₂) in a combination of MeOH and benzene (Scheme 4, Table S1 in the Supporting Information).²¹

The carboxylic group was also transformed in urea derivatives by using the Curtius rearrangement (Scheme 5). Compound **1** was treated with diphenylphosphine azide (DPPA) to form an active carbonyl azide which boiled in toluene, losing N₂ to give isocyanate **35**.²² Derivative **35** was next reacted with the corresponding amine to give urea **36**, **37**, **38**, **39**, and **40**.²³ Amines used during the Curtius

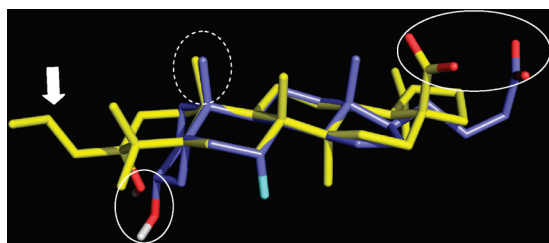


Figure 2. Superposition of **18 dia 1** (C, O, and polar H atoms in yellow, red, and white, respectively) and **7α-F-lithocholic acid** (C, O, F, and polar H atoms in blue, red, light blue, and white, respectively). Key polar chemotypes are circled with a white line; putative hydrophobic interacting groups are circled with a dashed line; allyl moiety is indicated by an arrow.

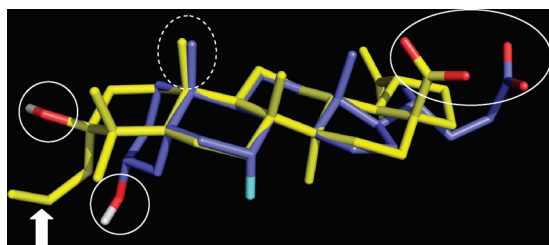


Figure 3. Superposition of **18 dia 2** (C, O, and polar H atoms in yellow, red, and white, respectively) and **7α-F-lithocholic acid** (C, O, F, and polar H atoms in blue, red, light blue, and white, respectively). Key polar chemotypes are circled with a white line; putative hydrophobic interacting groups are circled with a dashed line; allyl moiety is indicated by an arrow.

rearrangement to produce analogues **36**, **37**, **39**, and **40** correspond also to the one used in the amide series **23**, **32**, **31**, and **29**.

Modifications on the Alkene Function: (Scheme 6). Finally, we investigated the effect of alkene modification on TGR5 following the synthetic route shown in Scheme 6. Betulinic acid was hydrogenated to alkane **41**.¹⁸ Then, **1** was reacted with *meta*-chloroperoxybenzoic acid (mCPBA) in THF to form the desired epoxide **42**.¹⁰ Hydroboration with boron hydride (BH₃) in THF followed by oxidative workup afforded the alcohol **43**,²⁴ and finally ozonolysis of **1** in CHCl₃/MeOH followed by reductive workup with dimethylsulfur has provided **44**²⁵ (Scheme 6).

Ligand-Based Modeling. To gain further insight into molecular recognition features of the terpenoid series we compared TGR5 ligands. Superposition of **18 dia 1** and of **18 dia 2** with **7α-F-lithocholic acid**, a potent molecule from the bile acid series (EC₅₀ = 0.25 μM; eff. = 99%),¹⁰ emphasized the 3D orientation of chemical functions necessary to binding TGR5 receptor (Figures 2 and 3). Interestingly, additional chemical groups like methyl at C-10 show a similar location suggesting that they also participate in ligand binding interaction. Moreover, the presence of the allyl at the C-3 position in **18** is well tolerated (EC₅₀ = 0.43 μM; eff. = 116%) indicating that there is room for a stabilizing hydrophobic contact near the OH group.

Biological Effect of the TGR5 Agonist 18 dia 2. Among the 50 betulinic acid derivatives, **18 dia 2** was found to be the most potent TGR5 agonist *in vitro*. In a previous study, we demonstrated that oleanolic acid, the original triterpenoid extracted from *Olea europaea* leaves for its TGR5 agonist activity, decreases body weight and more specifically fat pad mass.¹¹ Since Watanabe et al. demonstrated that TGR5

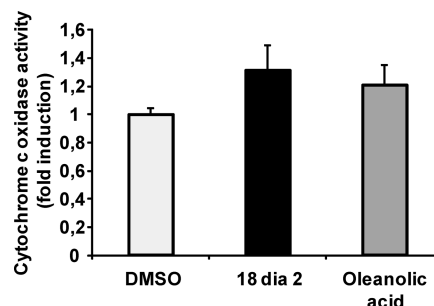


Figure 4. Mitochondrial effects of oleanolic acid and **18 dia 2** in 3T3L1 adipocyte cells. Mitochondrial activity as measured spectrophotometrically by cytochrome c oxidase assay in 3T3L1 adipocyte cells treated with the vehicle DMSO (white box), **18 dia 2** at 10 μM (black box), or oleanolic acid at 10 μM (gray box). Data represent means ± sd *n* = 8 for mitochondrial function.

Table 2. Body Weight and Biochemical Parameters

	high fat diet	
	vehicle	18 dia 2 30 mg/kg
body weight	1.03 ± 0.05	1.00 ± 0.04
ASAT	0.82 ± 0.04	0.63 ^a ± 0.07
ALAT	0.90 ± 0.06	0.59 ^a ± 0.08
glucose	1.75 ± 0.01	1.52 ± 0.18

^aData represent mean values relative to day 0 ± SEM, *n* = 10 animals/group (**p* < 0.05).

agonists increase mitochondrial function,⁶ an effect that could potentially explain the effect on adipose tissue through increased fat burning, we evaluated the effect of oleanolic acid and **18 dia 2** on mitochondrial activity in 3T3L1 cells. We demonstrated that oleanolic acid increases mitochondrial activity in adipocytes as demonstrated by the increase in cytochrome c oxidase activity (Figure 4). Furthermore, a stronger induction could be obtained with **18 dia 2**, emphasizing this molecule as a better TGR5 agonist. To evaluate its effect on metabolic disorders, a cohort of male C57BL/6J mice were fed a high fat (HF) diet (60% kcal fat) for 10 weeks to generate obese mice. Then, the food was supplemented with **18 dia 2** at a dose of 30 mg/kg/day for 3 weeks. The body weight, measured weekly, revealed no significant effect of the compound **18 dia 2** (Table 2). Although this new TGR5 agonist shows no effect on body weight, the plasma glucose level shows a tendency to decrease (1.75 ± 0.01 to 1.56 ± 0.18, relative to day 0 of treatment) after 3 weeks of **18 dia 2** administration (Table 2). The oral glucose tolerance test (OGTT) performed after 14 days of treatment did not show any significant effect of **18 dia 2**. Likewise, the evaluation of plasma cholesterol level and distribution of fat tissue (weighted after sacrifice) indicate no modification for the mice treated with **18 dia 2**.

In addition to being more potent than **2** *in vitro*, **18 dia 2** is also less cytotoxic since **2** presented some toxic effects *in vivo*, whereas **18 dia 2** showed no increase of serum liver enzymes levels (Table 2) and no decrease in food intake (data not shown). Although, **18 dia 2** is a potent TGR5 agonist *in vitro*, it lacked effects *in vivo*, which could be explained by the weak bioavailability of this hydrophobic molecule in the organism, a fact that also contributes to the reduced toxicity.

Discussion

In the present study, we focused on the development of selective TGR5 agonists from the triterpenoid family. In our

biological evaluation, selectivity between TGR5 and the FXR receptor was pointed out by triterpenoids which showed high TGR5/FXR selectivity. In contrast, certain bile acid derived TGR5 agonists show a dual effect on the two different receptors bile acid receptors, FXR and TGR5.⁹

In this work, a series of triterpenoids, which are representative of the structural diversity found in nature and covering the lupane, oleanane, ursane, lanostane, dammarane, friedlane, and cycloartane skeleton, were evaluated for their TGR5 agonist potency. In the sequence of the tested natural triterpenoids, the lupane, oleanane, and ursane subfamilies demonstrated activity on TGR5. Indeed, **1**, **2**, and ursolic acid (**3**) (Table 1) showed TGR5 agonist a potency greater than in the case of LCA with an EC₅₀ of 1.04, 2.25, and 1.43 μ M, respectively. All of them proved to be specific agonists of TGR5 with no activity on FXR even at the highest concentration tested (30 μ M). Interestingly, those three triterpenoids bear common features. They have a pentacyclic carbon skeleton, a hydroxyl group at C-3, and a carboxylic acid group at C-17. Triterpenoids **1**, **2**, and **3** show the same stereochemistry (*S*) at both the C-3 –OH and the C-17 –COOH. Noteworthy, **1**, **2**, and **3** also bear an alkene either at C-20 or at C-12.

Structural comparison between the active and the nonactive natural triterpenoids demonstrated the importance of the hydroxyl and the carboxylic acid at C-3 and C-17. Indeed, lupenone and friedline have shown a drop of activity, which may arise either from the oxidation of the C-3 hydroxyl group into a ketone or from absence of a carboxylic acid function, assuming that the hydroxyl group and/or the carboxylic acid have a key role in the given activities. The significance of the carboxylic acid for the TGR5 activity was underlined by the complete loss of activity of betulin and uvaol which differ from parent **1** and **3** only by reduction of the C-17 COOH into CH₂OH (Table 1). Additionally, the absence of carboxylic acid on the chemical structure of **3** exemplified by α -amyrin produced the same effect. Also, the lack of the ability from β -elemenic acid and β -glycyrrhetic acid to bind to the receptor should mean that all triterpenoids with hydroxyl and/or carboxylic acid are at different positions than C-3 and C-17 should not be inactive. Then, the value of having one free hydroxyl at C-3 was confirmed with the inactivity of arjulonic acid and asiatic acid: they share a similar scaffold to that of the active triterpenoids **2** and **3** but showed no activity at all. Thus, we assume that additional hydroxyl groups on the α and β position around the C-3 may disrupt some hydrophobic interactions or generate unfavorable steric constraints within the receptor. That is in line with the model proposed by Sato et al.,¹⁰ reporting a narrow pocket with hydrogen bond acceptor groups in this part of the TGR5 binding site, and suggests a similar location of the bile acid and the triterpenoid series within the receptor.

To gain further information on the receptor TGR5, we have chosen betulinic acid (**1**) as our lead compound for an SAR study. Indeed, **1** has retained our attention because of its better TGR5 agonist activity and efficacy *in vitro* compared to the other tested triterpenoids and to LCA (Table 1). We have investigated how **1** binds inside the active pocket of the protein by synthesizing ~50 analogues that differed at the hydroxyl and the carboxylic acid at C-3 and C-17 as well as at the C-20 alkene.

First, modification of the hydroxyl group into ester **4**, **5**, and **6** revealed a total loss of activity confirming the necessity of keeping the C-3 hydroxyl group for a first class TGR5 agonist

Table 3. Effects on the TGR5 Activity after Modifications on the Hydroxyl Group

name	TGR5		FXR
	EC ₅₀ , μ M	efficacy	
4	> 10	0	0
5	> 10	0	0
6	> 10	0	0
7	4.71	217	0
8	> 10	0	0
9	1.75	132	0
10	5.00	159	0
11	3.17	20	0
12	7.88	139	0
13	7.73	126	0
14	3.65	13	0
15	> 10	0	0
16	> 10	0	0
17	> 10	0	0
18 mixture dia 1/dia 2	0.43	116	0
18 dia 1	2.08	128	0
18 dia 2	0.12	122	0
19 mixture dia 1/dia 2	1.19	125	0
19 dia 1	6.27	67	0
19 dia 2	0.42	117	0

(Table 3). These results were anticipated with regards to the loss of activity previously observed with the natural triterpenoids (Table 1). Also, oxidation of the hydroxyl group into ketone decreases the activity (EC₅₀ = 4.71 μ M) highlighting the point that the hydrogen donor character of the hydroxyl group is required for the binding. The same conclusion was driven from analysis of the acetal derivative **8** and the methoxy derivative **15** which show no activity (Table 3). As confirmation of the statement of the hydrogen donor character requirement, only oxime **22** slightly lowers the TGR5 potency (EC₅₀ = 1.75 μ M) in contrast to ester (**4–6**) or oxime derivatives (**10–14**) which show a total loss of activity (Table 3).

Evaluation of these compounds showed that the relocation of the hydroxyl on oxime **22** is accepted even if it is not optimum. But, replacements of the C-3 hydroxyl group by any residue led to a loss of activity. These results indicated that the hydroxyl should keep its hydrogen donor feature, which is again in agreement with Macchiarulo et al., who predicted by molecular field analysis and 3D-quantitative the structure of a narrow hydrogen bond donor site around the C-3 position.⁹ Nevertheless, the binding site of this molecule needs more investigation as no prediction was realized with regards to the configuration at the C-3 carbon, such as **18 dia 2**, the most potent TGR5 agonist we have synthesized so far which gave exceedingly better activity. Indeed, we have observed a remarkable change when ketone **7** was subject to Grignard reaction. Two Grignard alkylations have been achieved by using an allylorganomagnesium (**18**) and a 2-methylallylorganomagnesium (**19**) reagent. Formation of the new chiral carbon by Grignard reaction gave two diastereoisomers each time with distinct activities **18/19 dia 1** and **18/19 dia 2** (Table 3). The allylic alkylation using a Grignard reagent gave better activity than the methylallylic alkylation for both diastereoisomers (Table 3). This difference can only be explained by the shape of the carbon side chain which may confer more steric hindrance for the methylallylic derivative. Indeed, both **18** and **19** stand with the same alkene functional group and only differ by the position of the alkene on the side chain carbon. The comparison of the two diastereoisomers on TGR5 indicated that the chiral configuration needs to be C-3

(*R*) for a good binding. Indeed, diastereoisomers of the (*R*) configuration at C-3 proved to be more potent in both cases with an EC_{50} value of 0.12 and 0.42 μ M for **18 dia 2** and **19 dia 2**, respectively. By comparison, **18 dia 1** and **19 dia 1** showed values of EC_{50} = 2.08 μ M and EC_{50} = 6.27 μ M, respectively. Efficiency increases accordingly for **18 dia 2** (eff. = 122%) and **19 dia 2** (eff. = 117%) (Table 3). Furthermore, diastereoisomers from **18** and **19** were mixed to obtain an equimolar mixture of **dia 1/dia 2**. The idea was to understand the behavior of the 1:1 mixture on the TGR5 receptor. The results have shown moderate to good activity with EC_{50} = 0.43 μ M and EC_{50} = 1.19 μ M, respectively, to **18** and **19**. In both **18** and **19** cases, the resulting activity appeared to be mainly driven by the most active diastereoisomer (**dia 2**) (Table 3).

Figure 3 displays the superposition of the most potent stereoisomer **18 dia 2** with an (*R*) C-3 OH in an equatorial position and a potent bile acid: surprisingly, the two molecules do not show an overall fit as good as the one deriving from the superposition of the less potent **18 dia 1** (Figure 2). It is noteworthy that the critical OH group of **18 dia 1** is close to the OH group of the bile acid, and that is no longer the case with **18 dia 2**. Altogether, these data suggest that the betulinic acid series locates in the vicinity of the bile acid series within the TGR5 binding site but using a specific orientation. This orientation might also be characterized by the presence of a hydrophobic pocket near the OH group since the allyl triterpene derivative **18** is a potent compound.

Finally, we are the first group to report the introduction of a carbon side chain at C-3, which increases the potency. These results confirm the recently reported enantiomeric selectivity of TGR5 toward enantiomeric BAs.²⁶

The results obtained when evaluating modifications of the carboxylic acid are consistent with the screening of the natural triterpenoids, which indicated that carboxylic acid should stay unchanged in its original position. Indeed, modification of the carboxylic acid was complicated, as transformation into esters (**20–23**), amides (**23–33**), isocyanate (**35**) and ureas (**36–40**) gave rise to inactive derivatives (Table S1 in the Supporting Information). Even the methyl ester analogue **25** did not activate the receptor. In fact, this study on the carboxylic acid made us aware of the essential attribute of the hydrogen donor character of COOH for a good binding.

As strong modifications drop the activity, we have raised the hypothesis of a small polar site recognizing the free carboxylic acid which rules the TGR5 activation. To the contrary, Sato et al. suggest a large binding pocket in this region of the receptor which can host the labile carboxylic acid side chain of BAs. This difference in results is probably due to the poor flexibility of the triterpenoid structures which cannot accommodate positioning in the binding site with regard to steric hindrance deriving from substitutions on carboxylic acid. Thus, it is conceivable that the difference in flexibility between the two series is linked to the selectivity toward TGR5. That assumption is in agreement with reported bioactive conformations of bile acid derivatives showing an extended carboxylic side chain (e.g., 6ethyl_chenodeoxycholic_acid; PDB entry 1OT7) required for building a salt bridge with an arginine residue within the FXR binding pocket (data not shown). The betulinic acid series does not possess any flexibility at this point and, consequently, would not form the necessary contacts with FXR interacting residues.

Further modification on the alkene demonstrates a weak effect on the activity, meaning that alkene is not involved in

Table 4. Effects on the TGR5 Activity after Modifications on the Alkene

name	TGR5		FXR
	EC_{50} , μ M	efficacy	
41	2.17	60	0
42	6.91	71	0
43	3.32	109	0
44	3.11	156	0

Table 5. Physicochemical Properties of **18 dia 2**^a

	18 dia 2	
	rules	properties
molecular weight	< 500 g/mol	496.8 g/mol
number of hydrogen bond acceptor (ON)	< 10	3
number of hydrogen bond donor (OH, NH)	< 5	2
partition coefficient (mi Log <i>P</i>)	< 5	8.03

^aData represent values calculated according to the Lipinski's rules.

the drug–receptor interaction. Indeed, the replacement of alkene by alkane **41** (EC_{50} = 2.17 μ M), epoxide **42** (EC_{50} = 6.91 μ M), hydroxyl group **43** (EC_{50} = 3.32 μ M), and ketone **44** (EC_{50} = 3.11 μ M) slightly lowers the activity, meaning that all those modifications appeared compatible with TGR5 activation (Table 4). This outcome led us to think that alkene is in the outer sphere of the binding pocket. This feature will be used in a future strategy to improve molecule solubility without losing the biological activity of our derivatives by transforming the alkene function to obtain a better biological tool. Indeed, triterpenoid are hydrophobic molecules, and this feature was a non-negligible disadvantage in our biological test. One of the goals of the synthesis of amide derivatives (**27–31**) was also the improvement of the solubility of **1** by addition of one or more hydroxyl groups on the side chain carbon. But all the compounds were inactive. During the examination of the physicochemical properties of **18** calculated through the use of the predictive Linspiski's rules, we noticed one violation among the four parameters predicted by the rules since the value of the partition coefficient log *P* is out of range (Table 5).²⁷ This feature represents poor bioavailability and is suspected to be the main cause of our disappointing *in vivo* data.

The importance of the chemical ring in drug discovery has been noticed as most of drugs contain rings in their structure. In our case rings have a multiple role, and more especially they induce the shape of the molecule and the special orientation of the critical polar groups. The common hydrophobic pentacyclic skeleton of the triterpenoids may also favor the biological binding with the active site via additional hydrophobic interactions. Indeed, the study by Sato et al. has already underlined this point previously by working with bile acids which also have a hydrophobic steroid skeleton. Indeed, they have predicted a hydrophobic pocket hosting the C-6 and C-7 position of BA steroid nucleus.⁹ The biological guided fractioning initially made to isolate the TGR5 active principle from *Olea europaea* only retained one hydrophobic compound from all the molecules contained in the leaves of the plant.

From a biological point of view this SAR has provided us with a very interesting tool compound, **18 dia 2**, which could contribute to the better understanding of the function of TGR5. However, this molecule could not be used successfully for *in vivo* testing probably because **18 dia 2** exhibited poor bioavailability as illustrated by the weak effects observed *in vivo*

despite the strong *in vitro* data. Indeed, previous pharmacokinetic studies performed on oleanolic acid have demonstrated that this molecule had a weak metabolic stability when administrated orally to rats.²⁸ In addition, in the same study, the bioavailability of this molecule was shown to be ~1%. In view of the close structural proximity of oleanolic acid and **18 dia 2** and the calculated log *P* of these molecules (6.7 and 8.2, respectively), it is most likely that **18 dia 2** exhibits the same poor pharmacokinetic properties. It will be of relevance to overcome this disadvantage in future studies when considering the nice *in vivo* data results obtained with **2** a close structural parent to **18 dia 2**. Although **2** had a weaker TGR5 potency *in vitro*, it had enhanced *in vivo* results when tested for its antidiabetic properties.¹⁰ Indeed, in an earlier study oleanolic acid has shown antihyperglycaemic abilities through enhancing the mitochondrial function by TGR5 activation,²⁹ an effect also seen with **18 dia 2** and confirmed in this work in adipocyte cells. Supported by various papers,⁶ we proposed a pathway that involves TGR5-D2-mitochondria or TGR5-PGC1-mitochondria. Additionally, more recently, it has been shown that oleanolic acid inhibits protein phosphatase 1B (PTP1B), a key regulator in the negative regulation of the insulin pathway.³⁰ Furthermore, oleanolic acid inhibits glycogen phosphorylase, which is responsible for the breakdown of glycogen to produce glucose.³¹ Altogether these results support the antidiabetic effect of oleanolic acid by different pathways, and future studies will be required to evaluate the activity of **18 dia 2** on these targets and determine if those effects are compound- and/or class-dependent. These biological data on **2** prompted us to look for a small structural arrangement on the triterpenoid skeleton of **18 dia 2** that might be beneficial to transforming it into a better *in vivo* therapeutic agent.

In this paper, we focused on BAs and triterpenoids as TGR5 agonists because of their similarities which are useful for comparisons. But, other classes of structure have appeared in the literature. Takeda Chemical Industry LTD has described the 6-methyl-2-oxo-4-thiophen-2-yl-1,2,3,4-tetrahydropyrimidine-5-carboxylic acid benzyl ester as a TGR5 agonist (yet we observed the product to be inactive).⁶ Nevertheless, this product was the first TGR5 agonist bringing structural diversity compared to the steroid shape of BAs and triterpenoids. Also, Kalypsys has disclosed a wide range of fused ring containing heteroatoms useful for the derivatization such as quinazolinone, quinoline, dihydropyridine, pyrrolo- and imidazodiazepine, purin, pyrazolo- and thienopyridine, and pyrido-, thieno-, and pyrazolopyrimidine.^{32–36}

Compounds were tested in a binary system in which an $EC_{50} < 10 \mu M$ compound was active and $EC_{50} > 10 \mu M$ compound was inactive. So, drawing a conclusion from this work was difficult, as most of the reported compounds have shown activity $EC_{50} < 10 \mu M$. Moreover, the selectivity of TGR5 agonists described by Takeda LTD and Kalypsys need to be proven. Indeed, the selectivity between TGR5 and FXR is not expressed in the different patents.

Conclusions and Perspectives

Triterpenoids represent a structurally novel class of TGR5 agonist. TGR5 is a recently identified G-protein coupled receptor which has drawn scientific attention in the field of metabolism. TGR5 agonists could be used to treat type 2 diabetes since its activation is capable of increasing the mitochondrial activity, whose deficiency is a hallmark of the

early stage of the disease. This positions TGR5 triterpenoid agonists as therapeutic agents for treating obesity and diabetes. To gain relevant pharmacological information on the TGR5 receptor, the discovery of potent and selective TGR5 agonists is of importance. An SAR study on several natural triterpenoids and more especially on betulinic acid derivatives has provided a highly potent TGR5 agonist, **18 dia 2** (RG-239). The first observation between all the potent agonists was the requirement of possessing a free hydroxyl and a free carboxylic acid. Considering that the hydroxyl and the carboxylic acid are key functional groups for the activation of TGR5, the possibility of including alkene modification for further experiments was raised. Further experiments will also take into account the ability of the TGR5 receptor to interact in a stereoselective manner with a potential agonist. Indeed, we demonstrated that the formation of a new chiral center at C-3 is one way to obtain highly potent betulinic acid derivatives.

Development of potent TGR5 agonists by this SAR has improved our knowledge on TGR5. Taken together these data reveal that the betulinic acid series has three main binding pockets: (a) a narrow hydrogen bond donor/acceptor site at the C-3 hydroxyl group, (b) a hydrophobic pocket hosting C-6 until C-9 and methyl pointing upward at C-10, (c) a small polar site recognizing the free carboxylic acid. By analyzing ligand superpositions, we highlighted a possible new arrangement around the C-3 binding pocket exemplified by the use of **18**. The selective binding pocket near the C-3 hydroxyl described by Sato et al. seems to be completed with an adjacent hydrophobic spot which participates in the improvement of potency of the betulinic acid series while maintaining selectivity toward TGR5.

Experimental Section

Chemistry General Procedure. Reaction conditions and yields were not optimized. Solvents were used dried and purified before use following the standard methodology. Flash chromatography was performed using silica gel (40–63 μm). NMR spectra were taken in $CDCl_3$ or C_5D_5N with a 5 mm Bruker probe that operates at 300 MHz (1H) and 75 MHz (^{13}C) or at 200 MHz (1H) and 50 MHz (^{13}C). 1H spectra in $CDCl_3$ were referenced to δ 7.26, while ^{13}C spectra in $CDCl_3$ were referenced to δ 77.23. Spectra 1H and ^{13}C taken in C_5D_5N were calibrated by reference to the first peak of pyridine at δ 7.22 and δ 123.87, respectively. IR spectra were recorded on a Thermo Electron Corporation FT-IR Spectrum spectrophotometer.

A. To a solution of oxime **9** (50 mg, 0.106 mmol, 1.0 equiv) in pyridine (0.5 mL), anhydride (0.16 mmol, 1.5 equiv) was added and then catalytic qualitative DMAP was added. The mixture was refluxed, cooled, and poured into a 5% HCl solution and then filtered and dried.

B. Compound **1** (50–150 mg, 0.11–0.33 mmol, 1.0 equiv) was dissolved in DMF (0.5–2 mL). Cs_2CO_3 (1.5 equiv) was added to the reaction mixture followed by an alkyl halide (1.5 equiv) at room temperature. After 5–16 h of stirring, the reaction mixture was poured in 10 mL of water. The resulting precipitate was filtered to give a white solid.

C. To a solution of **1** (50 mg, 0.11 mmol, 1.0 equiv) in DMF (0.5 mL) were added EDC (31 mg, 0.165 mmol, 1.5 equiv) and HOBT (22 mg, 0.165 mmol, 1.5 equiv). The solution was stirred at rt for 30 min whereupon diisopropylethylamine (29 μL , 0.165 mmol, 1.5 equiv) and the appropriate amine (0.165 mmol, 1.5 equiv) were added. The reaction mixture was allowed to stir for 12–20 h at rt. After this time the solution was poured in water. The resulting precipitate was filtered to give a white solid.

D. A solution of **1** (50 mg, 0.11 mmol, 1.0 equiv), DPPA (25 μL , 0.11 mmol, 1.0 equiv), and Et_3N (15 μL , 0.11 mmol, 1.0 equiv) in DMF (0.5 mL) was stirred at rt for 1 h. The solution of the resulting

azide was refluxed for 2 h. Then the solution containing the isocyanate was cooled to rt and treated with an excess of amine (10 equiv) before refluxing for 15 h. The resulting mixture was concentrated *in vacuo* and purified by silica gel column chromatography.

3-*O*-Succinyl-betulonic Acid (4). Compound **1** (50 mg, 0.11 mmol, 1.0 equiv) was heated with succinic anhydride (22 mg, 0.22 mmol, 2.0 equiv) in anhydrous pyridine (0.5 mL) to reflux overnight, under nitrogen. The reaction mixture was then poured into a mixture of dilute HCl 5% (20 mL) and stirred for 15 min. The precipitate obtained was filtered off and washed with water. The precipitate was chromatographed using a silica gel column (98/2 CHCl₃/MeOH) to afford the product **4** (21 mg, 35% yield) as a white amorphous powder. ¹H NMR (300 MHz, C₅D₅N) δ 0.75, 0.91, 0.96, 1.02, 1.07, 1.80 (each s, 3H, -CH₃), 0.66–2.03 (m, other aliphatic ring protons), 1.97 (s, 1H), 2.15–2.35 (m, 2H), 2.57–2.78 (m, 2H), 2.84–3.05 (m, 4H), 3.53 (br t, 1H, *J* = 9.0 Hz), 4.69–4.85 (m, 2H), 4.95 (s, 1H). ¹³C NMR (75 MHz, CDCl₃) δ 14.8, 16.3, 16.4, 16.7, 18.4, 19.5, 21.1, 23.8, 25.6, 25.8, 28.1, 29.4, 29.5, 29.8, 30.7, 32.3, 34.4, 37.3, 38.0, 38.5, 40.9, 42.6, 47.1, 49.4, 50.5, 55.6, 56.6, 68.1, 81.7, 109.9, 150.5, 172.0, 178.8, 183.4. MS (ESI-APCI) *m/z*: 439 (sc +), IR *v*_{max} cm⁻¹: 1704 and 1731 (C=O), 2870, 2932.

3-(Pent-4-enoyloxy)lup-20(29)-en-28-oic Acid (5). Compound **1** (50 mg, 0.11 mmol, 1.0 equiv) was dissolved in anhydrous pyridine (0.5 mL). 4-Pentenoic anhydride (80 μL, 0.44 mmol, 4.0 equiv) and DMAP (26 mg, 0.22 mmol, 2.0 equiv) were added, and the reaction mixture was refluxed under nitrogen for 5 h. The reaction mixture was acidified with HCl 5% and extracted with 5 mL of CHCl₃. The organic layer was washed with water and brine, dried over Na₂SO₄, and evaporated. The residue was purified by silica gel column chromatography (100% CHCl₃) to afford the product **5** (36 mg, 61% yield) as a white amorphous powder. ¹H NMR (200 MHz, CDCl₃) δ 0.82–0.89 (m, 9H, 3*CH₃), 0.94, 0.98, 1.70 (each s, 3H, -CH₃), 0.74–1.79 (m, other aliphatic ring protons), 1.89–2.07 (m, 2H), 2.10–2.34 (m, 2H), 2.36–2.45 (m, 4H), 2.94–3.09 (m, 1H), 4.49 (t, 1H, *J* = 9.8 Hz), 4.62 and 4.75 (br s, 1H each, on methylene group), 4.96–5.13 (m, 2H), 5.75–5.93 (m, 1H). ¹³C NMR (50 MHz, CDCl₃) δ 14.9, 16.3, 16.4, 16.8, 18.4, 19.6, 21.1, 24.0, 25.7, 28.2, 29.3, 29.9, 30.8, 32.4, 34.2, 34.5, 37.3, 37.4, 38.1, 38.6, 38.6, 40.9, 42.7, 47.1, 49.5, 50.6, 55.6, 56.6, 81.1, 111.0, 115.6, 137.0, 150.6, 173.1, 181.5. MS (ESI-APCI) *m/z*: 439 (sc +) and 537 (M - H)⁺ (sc -). IR *v*_{max} cm⁻¹: 1693 and 1730 (C=O).

3-(Isobutyryloxy)lup-20(29)-en-28-oic Acid (6). Compound **1** (50 mg, 0.11 mmol, 1.0 equiv) was dissolved in anhydrous pyridine (0.5 mL). Isobutyric anhydride (72 μL, 0.44 mmol, 4.0 equiv) and DMAP (26 mg, 0.22 mmol, 2.0 equiv) were added, and the reaction mixture was refluxed under nitrogen for 4 h. The reaction mixture was acidified with HCl 5% and extracted with 5 mL of CHCl₃. The organic layer was washed with water and brine, dried over Na₂SO₄, and evaporated. The residue was purified by silica gel column chromatography (100% CHCl₃) to afford the product **6** (44 mg, 76% yield) as a white amorphous powder. ¹H NMR (300 MHz, CDCl₃) δ 0.83–0.88 (m, 6H, 2*CH₃), 0.86, 0.94, 0.99, 1.70 (each s, 3H, -CH₃), 1.16 (d, 3H, *J* = 5 Hz), 1.19 (d, 3H, *J* = 5 Hz), 0.74–1.80 (m, other aliphatic ring protons), 1.88–2.07 (m, 2H), 2.37–2.11 (m, 2H), 2.54 (sp, 1H, *J* = 8.4 Hz), 2.93–3.11 (m, 1H), 4.47 (t, 1H, *J* = 8.4 Hz), 4.62 and 4.75 (br s, 1H each, on methylene group). ¹³C NMR (75 MHz, CDCl₃) δ 14.9, 16.2, 16.4, 16.7, 18.4, 19.1, 19.4, 19.6, 21.1, 23.9, 25.7, 28.2, 29.9, 28.2, 30.8, 32.4, 34.5, 34.7, 37.3, 37.4, 38.2, 38.5, 38.6, 40.9, 42.6, 47.2, 49.5, 50.6, 55.6, 56.6, 80.6, 110.0, 150.6, 177.1, 182.3. MS (ESI-APCI) *m/z*: 439 (sc +) and 525 (M - H)⁺ (sc -). IR *v*_{max} cm⁻¹: 1698 and 1731 (C=O).

Betulonic Acid (7). To a solution of compound **1** (100 mg, 0.22 mmol, 1.0 equiv) in anhydrous DMF (2 mL) was added a freshly prepared Jones' reagent (CrO₃ 1.1 mmol, H₂SO₄ (95%) 95 μL, and H₂O 400 μL) dropwise at 0 °C. The solution was stirred for 15 h at room temperature. The product was precipitated by the solution being poured into vigorously stirred H₂O, filtered, and

washed with H₂O. Column chromatography of the crude material over silica eluted with 100% CHCl₃ gave ketone **7** (83 mg, 83% yield) as a white amorphous powder. ¹H NMR (300 MHz, C₅D₅N) δ 0.82, 1.02, 1.05, 1.06, 1.14, 1.81 (each s, 3H), 0.92–2.55 (m, other aliphatic ring protons), 2.15–2.32 (m, 2H), 2.45–2.54 (m, 2H), 2.59–2.81 (m, 2H), 3.48–3.63 (m, 1H), 4.80 and 4.97 (s, 1H each, on methylene group). ¹³C NMR (75 MHz, C₅D₅N) δ 15.1, 16.3, 16.4, 19.8, 20.2, 21.5, 22.0, 26.4, 27.1, 30.6, 31.5, 33.1, 34.3, 34.7, 37.4, 37.9, 39.0, 40.1, 41.3, 43.2, 47.7, 48.1, 50.0, 50.5, 55.3, 57.0, 110.3, 151.6, 179.2, 216.9. MS (ESI-APCI) *m/z*: 437 and 455 (sc +) and 455 (M - H)⁺ (sc -). IR *v*_{max} cm⁻¹: 1683 and 1703 (C=O), 2867, 2940.

1-Isopropenyl-5α,5β,8,8,11α-pentamethyloctadecahydrospiro-[cyclopenta[α]chrysene-9,2'[1,3]dioxolane]-3α(1H)-carboxylic Acid (8). To a solution of compound **7** (50 mg, 0.11 mmol, 1.0 equiv) in benzene (0.5 mL) was added ethylene glycol (245 μL, 4.4 mmol, 4.0 equiv) and *p*-toluenesulfonic acid (2.0 mg, 0.006 mmol, 0.05 equiv). The mixture was stirred at rt for 15 h before being evaporated and purified by silica gel flash column chromatography (100% CHCl₃) to afford the product **8** (27 mg, 49% yield) as a white amorphous powder. ¹H NMR (300 MHz, CDCl₃) δ 0.83, 0.87, 0.91, 0.94, 0.99, 1.70 (each s, 3H, -CH₃), 0.75–2.35 (m, other aliphatic ring protons), 2.87–3.12 (m, 1H), 3.85–4.02 (m, 4H), 4.62 and 4.74 (br s, 1H each, on methylene group). ¹³C NMR (75 MHz, CDCl₃) δ 15.0, 16.2, 18.6, 19.6, 20.2, 21.1, 23.1, 25.7, 27.2, 29.9, 30.8, 32.4, 34.4, 37.3, 38.6, 40.9, 42.3, 42.7, 47.2, 49.5, 50.4, 53.6, 56.6, 64.9, 65.1, 109.8, 113.6, 150.8, 181.9. MS (ESI-APCI) *m/z*: 437, 453, 499 (M + H)⁺ (sc +) and 497 (M - H)⁺ (sc -). IR *v*_{max} cm⁻¹: 1652, 1742 (C=O), 2869, 2942, 3441.

3-(Hydroxyimino)lup-20(29)-en-28-oic Acid (9). Compound **7** (30 mg, 0.07 mmol, 1.0 equiv) was dissolved in anhydrous pyridine (0.5 mL). Hydroxylamine hydrochloride (32 mg, 0.46 mmol, 6.6 equiv) was added, and the reaction mixture was refluxed under nitrogen for 4 h. The reaction mixture was acidified with HCl 5% and extracted with 5 mL of CHCl₃. The organic layer was washed with water and brine, dried over Na₂SO₄, and evaporated. The residue was purified on a silica gel column with 100% CHCl₃ to afford the product **9** (19 mg, 61% yield) as a white amorphous powder. ¹H NMR (300 MHz, C₅D₅N) δ 0.89, 1.05, 1.07, 1.14, 1.38, 1.80 (each s, 3H, -CH₃), 0.80–2.04 (m, other aliphatic ring protons), 2.16–2.37 (m, 2H), 2.38–2.54 (m, 1H), 2.59–2.86 (m, 2H), 3.33–3.47 (m, 1H), 3.48–3.64 (m, 1H), 4.79 and 4.96 (s, 1H each, on methylene group). ¹³C NMR (50 MHz, C₅D₅N) δ 15.1, 16.2, 16.6, 17.8, 19.7, 19.8, 21.8, 23.8, 26.4, 28.3, 30.6, 31.5, 33.2, 34.7, 37.8, 38.0, 39.0, 39.5, 40.6, 41.4, 43.2, 48.1, 50.0, 51.0, 56.3, 57.0, 110.3, 151.6, 164.7, 179.3, 182.8. MS (ESI-APCI) *m/z*: 470 (M + H)⁺ (sc +) and 468 (sc -). IR *v*_{max} cm⁻¹: 1692 (C=O), 2867, 2940.

3-[(Acetyloxy)imino]lup-20(29)-en-28-oic Acid (10). Using general procedure A, oxime **9** (50 mg, 0.106 mmol, 1.0 equiv), acetic anhydride (12 μL, 0.160 mmol, 1.5 equiv), and DMAP (3 mg, 0.024 mmol, 0.2 equiv) in pyridine (0.5 mL) were refluxed overnight. The residue obtained was purified by silica gel column chromatography using 99/1 CHCl₃/MeOH to afford the product **10** (35 mg, 65% yield) as a white amorphous powder. ¹H NMR (300 MHz, CDCl₃) δ 0.89–1.04 (m, 9H, 3*CH₃), 1.20, 1.24, 1.70 (each s, 3H, -CH₃), 2.18 (s, 3H, -CH₃), 0.70–2.58 (m, other aliphatic ring protons), 2.72–3.12 (m, 1H), 4.62 and 4.75 (br s, 1H each, on methylene group). ¹³C NMR (75 MHz, CDCl₃) δ 14.8, 16.1, 16.3, 19.2, 19.6, 19.7, 20.3, 21.4, 22.9, 25.7, 27.5, 29.8, 30.7, 32.3, 34.0, 37.2, 37.4, 38.7, 39.2, 40.9, 41.5, 42.7, 47.1, 49.4, 50.3, 55.6, 56.6, 110.0, 150.6, 170.1, 175.1, 182.2. MS (ESI-APCI) *m/z*: 406, 452 (sc +) and 510 (M - H)⁺ (sc -). IR *v*_{max} cm⁻¹: 880, 921, 1197, 1215, 1367, 1457, 1638, 1690, 1732, and 1769 (C=O), 2869, 2947, 3068.

(5β,8α,14β,18β,19β)-3-[(Benzoyloxy)imino]lup-20(29)-en-28-oic Acid (11). Using general procedure A, oxime **9** (50 mg, 0.106 mmol, 1.0 equiv), benzoic anhydride (36 mg, 0.160 mmol, 1.5 equiv) and DMAP (3 mg, 0.024 mmol, 0.2 equiv) in pyridine (0.5 mL) were refluxed overnight. The residue obtained was

purified twice by silica gel column chromatography using 99/1 CHCl₃/MeOH to afford a white amorphous powder as a mixture with a high percentage of product **11** (47 mg, 78% yield). ¹H NMR (200 MHz, CDCl₃): δ 0.93–1.02 (m, 9H, 3*CH₃), 1.20, 1.33, 1.70 (each s, 3H, –CH₃), 0.60–2.68 (m, other aliphatic ring protons), 2.83–3.14 (m, 2H), 4.62 and 4.75 (br s, 1H, each on methylene group), 7.39–7.65 (m, 3H), 8.07 (d, 2H, *J* = 7.4 Hz). ¹³C NMR (50 MHz, CDCl₃): δ 14.8, 16.2, 16.3, 19.2, 19.5, 20.2, 21.4, 22.8, 23.0, 23.2, 25.6, 27.6, 29.8, 30.8, 32.3, 34.0, 37.2, 37.4, 38.6, 39.3, 40.9, 41.8, 42.7, 47.1, 49.4, 50.3, 55.6, 56.6, 109.9, 128.6, 129.7, 129.9, 133.1, 150.5, 164.5, 176.6, 182.7. MS (ESI-APCI) *m/z*: 406, 452, 574 (M + H)⁺ (sc +). IR *v*_{max} cm^{−1}: 707, 1261, 1451, 1695 and 1743 (C=O), 2869, 2949, 3243.

(5β,8α,14β,18β,19β)-3-[(Pent-4-enoyloxy)imino]lup-20(29)-en-28-oic Acid (12). Using general procedure A, oxime **9** (50 mg, 0.106 mmol, 1.0 equiv), 4-pentenoic anhydride (19 μL, 0.160 mmol, 1.5 equiv), and DMAP (3 mg, 0.024 mmol, 0.2 equiv) in pyridine (0.5 mL) were refluxed overnight. The residue obtained was purified twice by silica gel column chromatography using 100% CHCl₃ to afford a white amorphous powder as a mixture with a high percentage of product **12** (43 mg, 74% yield). ¹H NMR (200 MHz, CDCl₃): δ 0.89–1.00 (m, 9H, 3*CH₃), 1.12, 1.24, 1.70 (each s, 3H, –CH₃), 0.64–2.64 (m, other aliphatic ring protons), 2.73–3.15 (m, 2H), 4.62 and 4.74 (br s, 1H, each on methylene group), 4.95–5.20 (m, 2H), 5.75–6.00 (m, 1H). ¹³C NMR (75 MHz, CDCl₃): δ 14.8, 16.1, 16.2, 19.2, 19.6, 19.8, 21.4, 22.8, 25.6, 27.5, 29.0, 29.8, 30.8, 32.3, 32.7, 34.0, 37.2, 37.4, 38.6, 2*CH₃, 39.2, 40.9, 41.6, 42.7, 47.1, 49.4, 50.3, 55.6, 56.6, 109.9, 129.9, 155.8, 150.6, 171.6, 175.4, 182.4. MS (ESI-APCI) *m/z*: 406, 452 (sc +) and 550 (M – H)⁺ (sc –). IR *v*_{max} cm^{−1}: 881, 1151, 1454, 1641, 1694, and 1759 (C=O), 2869, 2948, 3075.

(5β,8α,1β,18β,19β)-3-[(Propionyloxy)imino]lup-20(29)-en-28-oic Acid (13). Using general procedure A, oxime **9** (50 mg, 0.106 mmol, 1.0 equiv), propionic anhydride (20 μL, 0.160 mmol, 1.5 equiv), and DMAP (3 mg, 0.024 mmol, 0.2 equiv) in pyridine (0.5 mL) were refluxed overnight. The crude product was purified by silica gel column chromatography using 100% CHCl₃ to afford a mixture of product **13** (72 mg, 86% yield) as a white amorphous powder. ¹H NMR (300 MHz, CDCl₃): δ 0.95–1.00 (m, 6H, 2*CH₃), 1.21 (t, 3H, *J* = 7.5 Hz), 0.93, 1.12, 1.24, 1.70 (each s, 3H, –CH₃), 0.69–2.42 (m, other aliphatic ring protons), 2.47 (q, 2H, *J* = 7.5 Hz), 2.77–2.90 (m, 1H), 2.95–3.08 (m, 1H), 4.62 and 4.75 (br s, 1H, each on methylene group). ¹³C NMR (75 MHz, CDCl₃): δ 9.4, 14.8, 16.3, 19.2, 19.6, 19.7, 21.5, 23.0, 25.7, 26.8, 27.5, 27.6, 29.9, 30.8, 32.4, 34.0, 37.3, 37.4, 38.7, 39.2, 41.9, 41.6, 42.7, 47.1, 49.4, 50.3, 55.7, 56.6, 110.0, 150.6, 173.2, 175.2, 182.0. MS (ESI-APCI) *m/z*: 406, 452 (sc +) and 524 (M – H)⁺ (sc –). IR *v*_{max} cm^{−1}: 880, 1155, 1175, 1460, 1691 and 1761 (C=O), 2869, 2945.

(5β,8α,14β,18β,19β)-3-[(Isobutyryloxy)imino]lup-20(29)-en-28-oic Acid (14). Using general procedure A, oxime **9** (50 mg, 0.106 mmol, 1.0 equiv), isobutyric anhydride (26 μL, 0.160 mmol, 1.5 equiv), and DMAP (3 mg, 0.024 mmol, 0.2 equiv) in pyridine (0.5 mL) were refluxed overnight. The crude product was purified by silica gel column chromatography using 100% CHCl₃ to afford the product **14** (36 mg, 63% yield) as a white amorphous powder. ¹H NMR (300 MHz, CDCl₃): δ 1.00–0.91 (m, 9H, 3*CH₃), 1.21–1.29 (m, 9H, 3*CH₃), 1.13, 1.69 (each s, 3H, –CH₃), 0.69–2.14 (m, other aliphatic ring protons), 2.15–2.48 (m, 4H), 2.70 (septuplet, 1H, *J* = 6.8 Hz), 2.76–2.91 (m, 1H), 2.96–3.09 (m, 1H), 4.61 and 4.74 (br s, 1H, each on methylene group). ¹³C NMR (50 MHz, CDCl₃): δ 14.8, 16.1, 16.2, 19.2, 19.3, 2*CH₃, 19.6, 19.8, 21.4, 22.9, 25.7, 27.5, 29.9, 30.8, 32.3, 33.4, 34.0, 37.2, 37.4, 38.6, 39.3, 40.9, 41.6, 42.7, 47.1, 49.4, 50.3, 55.7, 56.6, 109.9, 150.6, 175.0, 175.8, 181.5. MS (ESI-APCI) *m/z*: 406, 452 (sc +) and 538 (M – H)⁺ (sc –). IR *v*_{max} cm^{−1}: 886, 1100, 1127, 1148, 1182, 1387, 1463, 1695 and 1757 (C=O), 2870, 2947.

3-Methoxylup-28-oic Acid (15). To a stirred solution of **1** (25 mg, 0.045 mmol, 1.0 equiv) in a mixture of THF/MeOH

(1/0.2 mL), Pd/C (10 mg) was added at rt under N₂ atmosphere. N₂ atmosphere was replaced by H₂ atmosphere. The reaction mixture was stirred for 12 h at rt, then filtrated through Celite, and washed with CHCl₃. The residue was purified over a silica gel column with 100% CHCl₃ to afford the product **15** (18 mg, 85% yield) as a white amorphous powder. ¹H NMR (300 MHz, CDCl₃): δ 0.82 (m, 3H, 1*CH₃), 0.87–0.91 (m, 6H, 2*CH₃), 0.97 (d, 3H, *J* = 7 Hz 1*CH₃), 1.04–1.11 (m, 9H, 3*CH₃), 1.21–1.66 (m, 16H), 1.68–2.04 (m, 7H), 2.14–2.26 (m, 1H), 2.60–2.85 (m, 4H), 3.35 (s, 3H). ¹³C NMR (50 MHz, C₅D₅N): δ 15.1, 15.3, 16.6, 16.8, 17.0, 19.9, 21.7, 22.8, 23.7, 23.8, 27.8, 28.6, 30.5, 30.6, 33.2, 35.2, 37.8, 38.3, 38.7, 39.0, 39.4, 41.5, 43.3, 45.2, 49.6, 51.0, 56.4, 57.4, 2*CH₃, 88.6, 179.3. MS (ESI-APCI) *m/z*: 395 and 441 (sc +) and 471 (M + H)⁺ (sc –). IR *v*_{max} cm^{−1}: 1101, 1691 (C=O), 2869, 2935.

Benzyl 3-Hydroxylup-20(29)-en-28-oate (16). Using general procedure B, **1** (50 mg, 0.11 mmol, 1.0 equiv), Cs₂CO₃ (54 mg, 0.16 mmol, 1.5 equiv), benzyl bromide (20 μL, 0.16 mmol, 1.5 equiv), DMF (2 mL) were combined in DMF. The crude product was directly chromatographed using a silica gel column using 9/1 cyclohexane/EtOAc as eluent to afford the product **16** (52 mg, 87% yield) as a white amorphous powder. ¹H NMR (200 MHz, CDCl₃): δ 0.76, 0.77, 0.81, 0.95, 0.96, 1.68 (each s, 3H, –CH₃), 0.56–2.06 (m, other aliphatic ring protons), 2.08–2.38 (m, 2H), 2.93–3.11 (m, 1H), 3.11–3.24 (m, 1H), 4.60 and 4.73 (br s, 1H each, on methylene group), 5.09 (d, 1H, *J* = 11.8 Hz), 5.17 (d, 1H, *J* = 11.8 Hz), 7.29–7.42 (m, 5H). ¹³C NMR (50 MHz, CDCl₃): δ 14.9, 15.6, 16.1, 16.4, 18.5, 19.6, 21.1, 25.8, 27.6, 28.2, 29.8, 30.8, 32.4, 34.5, 37.2, 37.4, 38.4, 38.9, 39.1, 40.9, 42.6, 47.2, 49.7, 50.8, 50.8, 55.5, 56.8, 66.0, C31, 79.2, 109.8, 128.2, 128.3, 128.5, 136.7, 150.8, 176.0. MS (ESI-APCI) *m/z*: 529, 547 (M + H)⁺ (sc +). IR *v*_{max} cm^{−1}: 2941, 2868, 1721 (C=O).

Benzyl 3-Methoxylup-20(29)-en-28-oate (17). Compound **16** (50 mg, 0.11 mmol, 1.0 equiv) was dissolved in anhydrous DMF (0.5 mL). Sodium hydride (15 mg, 0.625 mmol, 5.7 equiv) was added, and the reaction mixture was stirred for 2 h at rt before the addition of methyl iodide (14 μL, 0.230 mmol, 2.1 equiv). After 12 h of stirring, the reaction mixture was diluted with 60 mL of water and extracted three times with 15 mL of CHCl₃. The organic layer was washed with brine, dried, and evaporated. The residue was purified over a preparative plate using 99/1 CHCl₃/MeOH to afford the product **17** (26 mg, 51% yield) as a white amorphous powder. ¹H NMR (300 MHz, CDCl₃): δ 0.71–0.78 (m, 6H, 2*CH₃), 0.81 (each s, 3H, –CH₃), 0.99–0.91 (m, 6H, 2*CH₃), 1.69 (each s, 3H, –CH₃), 0.57–1.98 (m, other aliphatic ring protons), 2.10–2.37 (m, 2H), 2.54–2.71 (m, 1H), 2.93–3.11 (m, 1H), 2.35 (s, 3H), 4.60 and 4.73 (br s, 1H each, on methylene group), 5.09 (d, 1H, *J* = 12.2 Hz), 5.17 (d, 1H, *J* = 12.2 Hz), 7.29–7.42 (m, 5H). ¹³C NMR (50 MHz, CDCl₃): δ 14.9, 16.0, 16.3, 2*CH₃, 18.4, 19.6, 21.1, 22.4, 25.8, 28.2, 29.8, 30.8, 32.3, 34.5, 37.2, 37.4, 38.4, 38.8, 39.0, 40.9, 42.6, 47.2, 49.7, 50.8, 56.1, 56.8, 57.7, 65.9, 88.9, 109.8, 128.3, 128.4, 128.7, 136.7, 150.8, 176.0. MS (ESI-APCI) *m/z*: 437, 529, 561 (M + H)⁺ (sc +). IR *v*_{max} cm^{−1}: 1719 (C=O), 2933.

3-Allyl-3-hydroxylup-20(29)-en-28-oic Acid (18). To a solution of **7** (300 mg, 0.66 mmol, 1.0 equiv) in 30 mL of THF were added dropwise 660 μL (1.32 mmol, 2.0 equiv) of allyl magnesium bromide (2 M in THF) under argon at −78 °C. The reaction mixture was stirred at −78 °C for 2 h and then quenched with HCl 5%. The aqueous phase was extracted with CHCl₃, and the combined organic layers were dried over Na₂SO₄, filtered, and concentrated *in vacuo*. The crude product was purified by flash column chromatography (100% CHCl₃) to afford the product **18** (241 mg, 74%) as a white amorphous powder (**18 dia 1** 79 mg, 24%, **dia 18 dia 2** 162 mg, 49%).

18 Dia 1. ¹H NMR (200 MHz, CDCl₃): δ 0.79, 0.82, 0.92, 0.94, 0.99, 1.70 (s, each, 3H, –CH₃), 1.85 (s, 3H, –CH₃), 0.46–2.55 (m, other aliphatic ring protons), 2.92–3.13 (m, 1H), 4.62 and 4.74 (br s, 1H each, on methylene group), 5.05–5.21 (m, 2H),

5.83–6.00 (m, 1H). ^{13}C NMR (75 MHz, CDCl_3) δ 15.1, 15.9, 16.4, 19.1, 19.6, 20.8, 21.0, 23.8, 25.9, 29.4, 30.0, 30.9, 32.5, 34.7, 35.1, 37.3, 37.5, 38.8, 41.0, 41.1, 41.3, 42.8, 47.2, 49.7, 50.8, 51.4, 56.7, 75.3, 109.9, 118.9, 135.0, 150.7, 181.1. MS (ESI-APCI) m/z : 433, 479 (sc +) and 495 ($\text{M} - \text{H}$) $^+$ (sc -). IR ν_{max} cm^{-1} : 1687 ($\text{C}=\text{O}$), 2945, 3446.

18 Dia 2. ^1H NMR (300 MHz, CDCl_3) δ 0.84–0.90 (m, 9H, 3^*CH_3), 0.95, 1.01, 1.70 (each s, 3H, $-\text{CH}_3$), 0.76–1.80 (m, other aliphatic ring protons), 1.90–2.08 (m, 2H), 2.13–2.34 (m, 3H), 2.45–2.58 (m, 1H), 3.00 (dt, 1H, $J = 11.0$ Hz and $J = 4.3$ Hz), 4.62 and 4.75 (br s, 1H each, on methylene group), 5.07–5.21 (m, 2H), 5.82–5.99 (m, 1H). ^{13}C NMR (50 MHz, CDCl_3) δ 15.0, 16.3, 16.8, 19.1, 19.5, 19.6, 21.0, 24.3, 25.7, 28.8, 29.9, 30.8, 32.4, 34.7, 37.3 2^*C , 37.5, 37.8, 38.6, 41.0, 41.5, 42.7, 47.1, 49.5, 51.2, 53.4, 56.6, 76.5, 109.9, 118.3, 135.2, 150.6, 182.1. MS (ESI-APCI) m/z : 433, 479 (sc +) and 495 ($\text{M} - \text{H}$) $^+$ (sc -). IR ν_{max} cm^{-1} : 1687 ($\text{C}=\text{O}$), 2945, 3446.

(3 α ,5 β ,8 α ,14 β ,18 β ,19 β)-3-Hydroxy-3-(2-methylprop-2-en-1-yl)-lup-20(29)-en-28-oic Acid (19). To a solution of **7** (50 mg, 0.11 mmol, 1.0 equiv) in 5 mL of THF was added dropwise 1 mL (0.50 mmol, 4.5 equiv) of 2-methylallyl magnesium chloride (0.5 M in THF) under argon at -78°C . The reaction mixture was stirred at -78°C for 2 h and then quenched with HCl 5%. The aqueous phase was extracted with CHCl_3 , and the combined organic layers were dried over Na_2SO_4 , filtered, and concentrated *in vacuo*. The crude product was purified by silica gel column chromatography using 100% CHCl_3 to afford the two diastereoisomers of **19** (55 mg, 98%) as a white amorphous powder (**19 dia 1** 18 mg, 32%, **19 dia 2** 37 mg, 66%).

19 Dia 1. ^1H NMR (200 MHz, CDCl_3) δ 0.79, 0.82, 0.92, 0.94, 0.99, 1.70 (s, each, 3H, $-\text{CH}_3$), 1.85 (s, 3H), 0.46–2.55 (m, other aliphatic ring protons), 2.92–3.13 (m, 1H), 4.62 (s, 1H) 4.74 (s, 1H), 4.74 (s, 1H), 4.97 (s, 1H). ^{13}C NMR (75 MHz, CDCl_3) δ 15.0, 15.9, 16.3, 19.0 2^*C , 19.6, 23.9, 25.7, 26.2, 29.7, 29.9 2^*C , 30.8, 32.4, 34.6, 35.1, 37.3, 38.7, 40.9, 41.0, 42.7, 43.9, 47.2, 49.5, 50.6, 51.2, 53.4, 56.7, 75.3, 109.9, 115.4, 143.8, 150.7, 182.5. MS (ESI-APCI) m/z : 493 (sc +) and 509 ($\text{M} - \text{H}$) $^+$ (sc -). IR ν_{max} cm^{-1} : 884, 1375, 1456, 1689 ($\text{C}=\text{O}$), 2871, 2946, 3501.

19 Dia 2. ^1H NMR (300 MHz, CDCl_3) δ 0.85, 0.87, 0.88, 0.95, 1.01, 1.70 (s, each, 3H, $-\text{CH}_3$), 1.87 (s, 3H, $-\text{CH}_3$), 0.57–2.54 (m, other aliphatic ring protons), 2.95–3.10 (m, 1H), 4.61 (s, 1H), 4.74 (s, 1H), 4.77 (s, 1H), 4.93 (s, 1H). ^{13}C NMR (50 MHz, CDCl_3) δ 15.1, 16.4, 16.9, 19.2, 19.7 2^*C , 21.1, 24.4, 25.3, 25.9, 28.9, 30.0, 30.9, 32.5, 34.8, 37.3, 37.6, 38.2, 38.9, 41.0, 41.1, 41.9, 42.7, 47.2, 49.7, 51.4, 53.4, 56.7, 76.6, 109.9, 115.0, 144.2, 150.6, 181.7. MS (ESI-APCI) m/z : 493 (sc +) and 509 ($\text{M} - \text{H}$) $^+$ (sc -). IR ν_{max} cm^{-1} : 884, 1375, 1456, 1689 ($\text{C}=\text{O}$), 2871, 2946, 3501.

3-Hydroxylupan-28-oic Acid (41). Compound **1** (100 mg, 0.22 mmol, 1.0 equiv) was dissolved in a mixture of MeOH/THF (1/1 mL), and 10% Pd/C (30 mg) was added under a N_2 atmosphere. The N_2 atmosphere was replaced by a H_2 atmosphere. The reaction was stirred under a H_2 atmosphere for 24 h, then filtered through Celite, and washed with CHCl_3 to afford a white solid. The residue obtained was purified by silica gel column chromatography using 100% CHCl_3 to afford the product **41** (78 mg, 78% yield) as a white amorphous powder. ^1H NMR (200 MHz, $\text{C}_5\text{D}_5\text{N}$) δ 0.84–0.90 (m, 6H, 2^*CH_3), 0.95 (d, 3H, $J = 6.8$ Hz, CH_3), 1.02–1.10 (m, 9H, 3^*CH_3), 1.25 (s, 3H, CH_3), 0.68–2.06 (m, other aliphatic ring protons), 2.09–2.32 (m, 1H), 2.57–2.87 (m, 3H), 3.49 (t, 1H, $J = 7.8$ Hz, H-3). ^{13}C NMR (50 MHz, $\text{C}_5\text{D}_5\text{N}$) δ 15.2, 15.3, 16.8 2^*C , 19.2, 21.7, 23.7, 23.8, 27.9, 28.7, 29.1, 30.6, 30.7, 32.3, 33.2, 35.3, 37.9, 38.4, 38.8, 39.6, 39.9, 41.5, 43.4, 45.2, 49.6, 51.1, 56.3, 57.4, 78.5, 179.3. MS (ESI-APCI) m/z : 441 (sc +) and 457 ($\text{M} - \text{H}$) $^+$ (sc +). IR ν_{max} cm^{-1} : 1682 ($\text{C}=\text{O}$).

9-Hydroxy-5 α ,5 β ,8,8,11 α -pentamethyl-1-(2-methyloxiran-2-yl)-icosahydro-3 α H-cyclopenta[α]chrysene-3 α -carboxylic Acid (42). Compound **1** (50 mg, 0.11 mmol, 1.0 equiv) was dissolved in anhydrous THF (0.5 mL). The reaction was cooled to 0°C , and *meta*-chloroperbenzoic acid (mCPBA 70–80%) (38 mg, 0.22 mmol,

2.0 equiv) was added. The reaction mixture was stirred for 16 h, and the temperature was allowed to rise until rt by that time. The reaction mixture was diluted with sodium bisulphite and extracted with 5 mL of CHCl_3 . The organic layer was washed with water and brine, dried over magnesium sulfate, and evaporated. The residue was purified over a silica gel column with 100% CHCl_3 to afford the product **42** (32 mg, 61% yield) as a white amorphous powder. ^1H NMR (200 MHz, $\text{C}_5\text{D}_5\text{N}$) δ 0.87, 1.26, 1.35 (each s, 3H, $-\text{CH}_3$), 1.00–1.12 (m, 9H, 3^*CH_3), 0.74–2.88 (m, other aliphatic ring protons), 3.50 (t, 1H, $J = 7.7$ Hz). ^{13}C NMR (50 MHz, $\text{C}_5\text{D}_5\text{N}$) δ 15.2, 16.7 2^*C , 19.2, 19.3, 21.6, 27.7, 28.3, 28.7, 29.0, 30.4 2^*C , 33.1, 35.2, 37.8, 37.9, 38.2, 39.7, 39.9, 41.5, 43.2, 46.7, 50.7, 51.2, 56.3, 56.8, 57.3, 60.5, 78.5, 179.1. MS (ESI-APCI) m/z : 409, 455, 473 ($\text{M} + \text{H}$) $^+$ (sc +). IR ν_{max} cm^{-1} : 1681 ($\text{C}=\text{O}$).

29-Dihydroxylupan-28-oic Acid (43). To a solution of **1** (50 mg, 0.11 mmol, 1.0 equiv) in dry THF (0.7 mL) cooled at 0°C was added a 1 M solution of BH_3 in THF (0.13 mmol, 1.2 equiv). The reaction mixture was stirred at 0°C for 1 h and at rt for 16 h. After the solution was recooled to 0°C , 70 μL of ethanol, 25 μL of a saturated aqueous sodium acetate, and 35 μL of 30% hydrogen peroxide were added in that order. The mixture was stirred for 1 h at 0°C and for 19 h at rt, and then the solution was diluted with EtOAc and washed with water, dried over Na_2SO_4 , and concentrated *in vacuo*. The crude product was purified by flash column chromatography (99/1 $\text{CHCl}_3/\text{MeOH}$) to afford the product **43** (9 mg, 17% yield) as a white amorphous powder. ^1H NMR (300 MHz, $\text{C}_5\text{D}_5\text{N}$) δ 0.85, 1.24 (each s, 3H, $-\text{CH}_3$), 1.02–1.10 (m, 9H, 3^*CH_3), 1.28 (d, 3H, $J = 7.0$ Hz), 0.73–2.35 (m, other aliphatic ring protons), 2.59–2.71 (m, 1H), 2.71–2.91 (m, 2H), 3.49 (t, 1H, $J = 8.6$ Hz), 3.79 (t, 1H, $J = 10.0$ Hz), 4.22 (dd, 1H, $J = 4.4$ Hz and $J = 10.2$ Hz). ^{13}C NMR (75 MHz, $\text{C}_5\text{D}_5\text{N}$) δ 15.2, 16.7 2^*C , 16.8, 19.1, 19.4, 21.6, 24.9 2^*C , 28.1, 28.7, 29.0, 30.7, 33.2, 35.3, 37.8, 38.2, 39.0, 39.5, 39.6, 39.9, 41.5, 43.4, 44.5, 49.3, 51.1, 56.2, 57.4, 63.7, 78.5, 177.3. MS (ESI-APCI) m/z : 411, 457 (sc +). IR ν_{max} cm^{-1} : 756, 1040, 1454, 1688 ($\text{C}=\text{O}$), 2870, 2944, 3423.

1-Acetyl-9-hydroxy-5 α ,5 β ,8,8,11 α -pentamethylcosahydro-3 α H-cyclopenta[α]chrysene-3 α -carboxylic Acid (44). Compound **1** (50 mg, 0.11 mmol, 1.0 equiv) in DCM/MeOH (10 mL, 1v/1v) was ozonized. The resulting light yellow solution was quenched at -78°C with dimethylsulfur (22 μL , 0.29 mmol, 2.6 equiv) and stirred for 12 h from -78°C to rt. The solvent was removed, and the residual product was purified the first time with flash column chromatography (100% CHCl_3) and the second time over a preparative TLC plate (95/5 $\text{CHCl}_3/\text{MeOH}$) to afford the product **44** (34 mg, 34% yield) as a white amorphous powder. ^1H NMR (300 MHz, $\text{C}_5\text{D}_5\text{N}$) δ 0.83, 1.02, 1.04, 1.08, 1.10, 1.24, 2.24 (each s, 3H, $-\text{CH}_3$), 0.72–2.85 (m, other aliphatic ring protons), 3.46 (t, 1H, $J = 7.6$ Hz), 3.64–3.78 (m, 1H). ^{13}C NMR (75 MHz, $\text{C}_5\text{D}_5\text{N}$) δ 15.2, 16.7 3^*C , 19.1, 21.5, 28.1, 28.6, 29.0, 29.1, 30.0, 30.6, 32.7, 35.0, 37.7, 37.8, 38.1, 39.6, 39.9, 41.3, 43.0, 50.1, 51.2, 52.4, 56.2, 56.8, 78.4, 179.1, 212.0. MS (ESI-APCI) m/z : 441 (sc +) and 457 ($\text{M} - \text{H}$) $^+$ (sc -). IR ν_{max} cm^{-1} : 1716 ($2^*\text{C}=\text{O}$), 1318, 2944.

Ligand Based Modeling. Conformational analysis and superposition of conformers were performed using OMEGA and ROCS programs, respectively (OpenEye suite; www.eyesopen.com).

TGR5 Luciferase Assay. Chinese hamster ovary (CHO) cells were obtained from ATCC (Manassas, VA) and were maintained in minimum essential medium alpha (α -MEM) supplemented with 10% (V/V) fetal bovine serum (FBS), 100 μM nonessential amino acids (NEAA), 100 U/mL penicillin, and 100 $\mu\text{g}/\text{mL}$ streptomycin sulfate. For the TGR5 assay, a stable cell line was obtained by transfection of CHO cells TGR5 with 3.8 μg of TGR5 expression plasmid (pCMVSPORT6/TGR5), 3.8 μg of CRE-driven luciferase reporter plasmid (pCRE-Luc), and 0.4 μg of neomycin-resistant gene expression plasmid (pcDNA3.1(+)) using Lipofectamine 2000 reagent (Invitrogen, Cergy Pontoise, France). The transfected cells were selected with

100 $\mu\text{g/mL}$ G418 sulfate, and single clones were grown in a 96-well plate, independently. Samples were tested by luminescence on the CHO cell line transfected with a TGR5 plasmid expression. Then, TGR5 activity and efficiency were determined by a dose response curve covering a range of concentrations from 1 nM to 30 μM . The biological effects of triterpenoids on TGR5 were compared to those of lithocholic acid (LCA) used as an internal control in the luciferase assay. TGR5-expressing CHO cells were treated for 5 h with 10 μM lithocholic acid (LCA) or triterpenoids or triterpenoid derivatives, followed by a luciferase assay.³⁷ Luminescence was determined with CentroXS3 LB960 (Berthold Technologies, Bad Wildbad, Germany).

FXR Luciferase Assay. To evaluate the FXR activity of compounds, COS1 (ATCC) cells were transfected with 25 ng of hFXR expression plasmid (pCMX-hFXR), 25 ng of mouse (m) retinoid X receptor α (RXR α) expression plasmid (pCMX-mRXR α), 50 ng of reporter plasmid (pEcREx7-Luc), and 50 ng of pCMV β as an internal control in each well, using lipofectamine 2000 reagent. Approximately 18 h after transfections, cells were incubated for 5 h with different concentrations of each compound in fresh MEM (or DMEM). After this treatment, the cells were lysed and normalized luciferase activity were determined.³⁷

Cytochrome c Oxidase Assay. Mouse 3T3L1 cells were obtained from ATCC (Manassas, VA) and were maintained in DMEM supplemented with 10% (V/V) fetal bovine serum (FBS). Two days post-confluency, adipocyte differentiation was induced with a mixture of IBMX 500 μM , dexamethasone 1 μM , and insulin 10 $\mu\text{g/mL}$. After 7 days of differentiation, cells were treated with compounds and then lysed (20 mM HEPES, 0.1% Triton, 1 mM EDTA). Cell lysate was incubated with reduced cytochrome c (from equine heart, Sigma). The disappearance of reduced cytochrome c was followed spectrophotometrically at 550 nM (according to the manufacturer's instruction, Sigma).

Animals and Diet. Seven week old male C57BL/6J mice were purchased from Charles River. The high fat diet (60% kcal Fat, D12492) was purchased from Research Diet (New Brunswick, NJ). The mice were housed by 5 under controlled temperature and a 12 h light–dark cycle and had free access to food and water. The animals were kept for 10 weeks on the high fat diet ($n = 30$). After 10 weeks on high fat, the animals were divided into three groups of 10 animals: one group was kept on the high fat diet only, the second received the same food supplemented with the **18 dia 2** compound at a 30 mg/kg/day dose, and the third received the same food supplemented with oleanolic acid at a 50 mg/kg/day dose. The food intake was measured throughout the study, and the amount of drug was adjusted to keep the dosing stable. Body weight and food intake were determined every week. The experiment was carried out according to the ethical guidelines.

Acknowledgment. Work in the laboratories from the authors is supported by grants from Région Alsace, ULP, CNRS, INSERM, Hôpitaux universitaires de Strasbourg, EPFL, SNF, and Novalix. We would like to thank Dr. Adam P. and Pr. Rohmer M. for providing most of the natural triterpenoids and Dr. Pascal Muller and Laurent Hoeffler for their input in the ligand-based modelling studies.

Supporting Information Available: Table S1 concerning the effect on TGR5 activity after modifications on the carboxylic group; Detailed procedure for the synthesis of derivatives **20** to **40**; Description of the HPLC methods and purity values of all, natural and hemisynthetic products. This material is available free of charge via Internet at <http://pubs.acs.org>

References

- (1) Wild, S.; Roglic, G.; Green, A.; Sicree, R.; King, H. Global prevalence of diabetes: estimates for the year 2000 and projections for 2030. *Diabetes Care* **2004**, *27*, 1047–53.
- (2) Petersen, K. F.; Dufour, S.; Befroy, D.; Garcia, R.; Shulman, G. I. Impaired mitochondrial activity in the insulin-resistant offspring of patients with type 2 diabetes. *N. Engl. J. Med.* **2004**, *350*, 664–71.
- (3) Qiao, L.; Han, S. I.; Fang, Y.; Park, J. S.; Gupta, S.; Gilfor, D.; Amorino, G.; Valerie, K.; Sealy, L.; Engelhardt, J. F.; Grant, S.; Hylemon, P. B.; Dent, P. Bile acid regulation of C/EBP β , CREB, and c-Jun function, via the extracellular signal-regulated kinase and c-Jun NH₂-terminal kinase pathways, modulates the apoptotic response of hepatocytes. *Mol. Cell. Biol.* **2003**, *23*, 3052–66.
- (4) Wang, H.; Chen, J.; Hollister, K.; Sowers, L. C.; Forman, B. M. Endogenous bile acids are ligands for the nuclear receptor FXR/BAR. *Mol. Cell* **1999**, *3*, 543–53.
- (5) Itoh, F.; Hinuma, S.; Kanzaki, N.; Miki, T.; Kawamata, Y.; Oi, S.; Tawaraishi, T.; Ishichi, Y.; Hirohashi, M. Preparation of aromatic ring-fused cyclic compounds as TGR5 receptor agonists. 2004-JP706 2004067008, 20040127, **2004**.
- (6) Watanabe, M.; Houten, S. M.; Matak, C.; Christoffolete, M. A.; Kim, B. W.; Sato, H.; Messaddeq, N.; Harney, J. W.; Ezaki, O.; Kodama, T.; Schoonjans, K.; Bianco, A. C.; Auwerx, J. Bile acids induce energy expenditure by promoting intracellular thyroid hormone activation. *Nature* **2006**, *439*, 484–9.
- (7) Maruyama, T.; Tanaka, K.; Suzuki, J.; Miyoshi, H.; Harada, N.; Nakamura, T.; Miyamoto, Y.; Kanatani, A.; Tamai, Y. Targeted disruption of G protein-coupled bile acid receptor 1 (Gpbar1/M-Bar) in mice. *J. Endocrinol.* **2006**, *191*, 197–205.
- (8) Katsuma, S.; Hirasawa, A.; Tsujimoto, G. Bile acids promote glucagon-like peptide-1 secretion through TGR5 in a murine enteroendocrine cell line STC-1. *Biochem. Biophys. Res. Commun.* **2005**, *329*, 386–90.
- (9) Sato, H.; Macchiarulo, A.; Thomas, C.; Gioiello, A.; Une, M.; Hofmann, A. F.; Saladin, R.; Schoonjans, K.; Pellicciari, R.; Auwerx, J. Novel potent and selective bile acid derivatives as TGR5 agonists: biological screening, structure-activity relationships, and molecular modeling studies. *J. Med. Chem.* **2008**, *51*, 1831–41.
- (10) Takikawa, H.; Hirooka, M.; Sasaki, M. The first synthesis of (Δ^5)-brevione B, an allelopathic agent isolated from *Penicillium* sp. *Tetrahedron Lett.* **2003**, *44*, 5235–5238.
- (11) Kashiwada, Y.; Hashimoto, F.; Cosentino, L. M.; Chen, C. H.; Garrett, P. E.; Lee, K. H. Betulinic acid and dihydrobetulinic acid derivatives as potent anti-HIV agents. *J. Med. Chem.* **1996**, *39*, 1016–7.
- (12) Dess, D. B.; Martin, J. C. A useful 12-I-5 triacetoxypiperidine (the Dess–Martin piperidine) for the selective oxidation of primary or secondary alcohols and a variety of related 12-I-5 species. *J. Am. Chem. Soc.* **1991**, *113*, 7277–87.
- (13) Roy, J.; Breton, R.; Martel, C.; Labrie, F.; Poirier, D. Chemical synthesis and biological activities of 16 β -derivatives of 5 β -androstane-3 β ,17 β -diol as antiandrogens. *Bioorg. Med. Chem.* **2007**, *15*, 3003–3018.
- (14) Tsukahara, M.; Nishino, T.; Furuhashi, I.; Inoue, H.; Sato, T.; Matsumoto, H. Synthesis and inhibitory effect of novel glycyrrhetic acid derivatives on IL-1 β -induced prostaglandin E₂ production in normal human dermal fibroblasts. *Chem. Pharm. Bull.* **2005**, *53*, 1103–1110.
- (15) Liu, D.; Song, D.; Guo, G.; Wang, R.; Lv, J.; Jing, Y.; Zhao, L. The synthesis of 18 β -glycyrrhetic acid derivatives which have increased antiproliferative and apoptotic effects in leukemia cells. *Bioorg. Med. Chem.* **2007**, *15*, 5432–5439.
- (16) Tchédam Ngatcha, B.; Luu-The, V.; Labrie, F.; Poirier, D. Androstosterone 3 β -ether-3 β -substituted and androstosterone 3 β -substituted derivatives as inhibitors of type 3 17 β -hydroxysteroid dehydrogenase: Chemical synthesis and structure–activity relationship. *J. Med. Chem.* **2005**, *48*, 5257–5268.
- (17) Bloch, R.; Gilbert, L. Synthesis of both enantiomers of 1 β -substituted 1 β ,1 β -unsaturated 1 β -lactones. *J. Org. Chem.* **1987**, *52*, 4603–5.
- (18) Imahori, T.; Ojima, H.; Yoshimura, Y.; Takahata, H. Acceleration effect of an allylic hydroxy group on ring-closing enyne metathesis of terminal alkynes: scope, application, and mechanistic insights. *Chem.—Eur. J.* **2008**, *14*, 10762–10771.
- (19) Wen, X.; Sun, H.; Liu, J.; Wu, G.; Zhang, L.; Wu, X.; Ni, P. Pentacyclic triterpenes. Part 1: The first examples of naturally occurring pentacyclic triterpenes as a new class of inhibitors of glycogen phosphorylases. *Bioorg. Med. Chem. Lett.* **2005**, *15*, 4944–4948.
- (20) Gaucher, A.; Wakselman, M.; Mazaleyra, J.-P.; Crisma, M.; Formaggio, F.; Toniolo, C. 1 β -Homo-peptides built from 1 β ,2 β -HBip, a biphenyl-substituted 3-amino-2,2-dimethylpropanoic acid. *Tetrahedron* **2000**, *56*, 1715–1723.

- (21) Liu, X.; Hu, X. E.; Tian, X.; Mazur, A.; Ebetino, F. H. Enantioselective synthesis of phosphinyl peptidomimetics via an asymmetric Michael reaction of phosphinic acids with acrylate derivatives. *J. Organomet. Chem.* **2002**, *646*, 212–222.
- (22) Ravn Matthew, M.; Peters Reuben, J.; Coates Robert, M.; Croteau, R. Mechanism of abietadiene synthase catalysis: stereochemistry and stabilization of the cryptic pimarenyl carbocation intermediates. *J. Am. Chem. Soc.* **2002**, *124*, 6998–7006.
- (23) Reynolds, R. C.; Johnson, C. A.; Piper, J. R.; Sirotnak, F. M. Synthesis and antifolate evaluation of the aminopterin analogue with a bicyclo[2.2.2]octane ring in place of the benzene ring. *Eur. J. Med. Chem.* **2001**, *36*, 237–242.
- (24) Ferraz, H. M. C.; Souza, A. J. C.; Tenius, B. S. M.; Bianco, G. G. Total synthesis of the sesquiterpenes beta -corymbolol and corymbolone. *Tetrahedron* **2006**, *62*, 9232–9236.
- (25) Bunnelle, W. H.; Rafferty, M. A.; Hodges, S. L. Aldol-equivalent elaboration of sterically hindered ketones: methallylmagnesium chloride as a synthon for acetone enolate. *J. Org. Chem.* **1987**, *52*, 1603–5.
- (26) Katona, B. W.; Cummins, C. L.; Ferguson, A. D.; Li, T.; Schmidt, D. R.; Mangelsdorf, D. J.; Covey, D. F. Synthesis, characterization, and receptor interaction profiles of enantiomeric bile acids. *J. Med. Chem.* **2007**, *50*, 6048–58.
- (27) Lipinski, C. A.; Lombardo, F.; Dominy, B. W.; Feeney, P. J. Experimental and computational approaches to estimate solubility and permeability in drug discovery and development settings. *Adv Drug Deliv Rev* **2001**, *46*, 3–26.
- (28) Jeong, D. W.; Kim, Y. H.; Kim, H. H.; Ji, H. Y.; Yoo, S. D.; Choi, W. R.; Lee, S. M.; Han, C. K.; Lee, H. S. Dose-linear pharmacokinetics of oleanolic acid after intravenous and oral administration in rats. *Biopharm. Drug. Dispos.* **2007**, *28*, 51–7.
- (29) Strehle, A.; Sato, H.; Genet, C.; Thomas, C.; Lobstein, A.; Wagner, A.; Auwerx, J.; Saladin, R. In *Characterization of the effect of a TGR5 agonist isolated from Olea Europaea on metabolic disorders*, Molecules et ingrédients Santé 2008, 3e colloque européen Rennes, 2008; Rennes, 2008.
- (30) Zhang, Y. N.; Zhang, W.; Hong, D.; Shi, L.; Shen, Q.; Li, J. Y.; Li, J.; Hu, L. H. Oleanolic acid and its derivatives: new inhibitor of protein tyrosine phosphatase 1B with cellular activities. *Bioorg. Med. Chem.* **2008**, *16*, 8697–705.
- (31) Chen, J.; Gong, Y.; Liu, J.; Hua, W.; Zhang, L.; Sun, H. Synthesis and biological evaluation of novel pyrazolo[4,3-b]oleanane derivatives as inhibitors of glycogen phosphorylase. *Chem. Biodiversity* **2008**, *5*, 1304–12.
- (32) Herbert, M. R.; Pinkerton, A. B.; Siegel, D. L. Preparation of pyridine containing heterocyclic compounds as TGR5 agonists. 2008-188789 2009054304, 20080808., **2009**.
- (33) Pinkerton, A. B.; Kabakibi, A.; Gahman, T. C. Preparation of diazepines and other heterocyclic modulators of TGR5 for treating metabolic, cardiovascular, and inflammatory diseases. 2007-US85267 2008067222, 20071120., **2008**.
- (34) Pinkerton, A. B.; Kabakibi, A.; Herbert, M. R.; Siegel, D. L. Preparation of quinoline compounds as modulators of TGR5 for treatment of disease. 2008-US53056 2008097976, 20080205., **2008**.
- (35) Pinkerton, A. B.; Kabakibi, A.; Hoffman, T. Z.; Siegel, D. L.; Noble, S. A. Preparation of quinazolinone modulators of TGR5 for treatment of metabolic, cardiovascular and inflammatory diseases. 2007-US85225 2008067219, 20071120., **2008**.
- (36) Smith, N. D.; Payne, J. E.; Hoffman, T. Z.; Bonnefous, C.; Pinkerton, A. B.; Siegel, D. L. Preparation of pyrimidine derivatives as TGR5 agonists. 2008-US73501 2009026241, 20080818., **2009**.
- (37) Picard, F.; Gehin, M.; Annicotte, J.; Rocchi, S.; Champy, M. F.; O'Malley, B. W.; Chambon, P.; Auwerx, J. SRC-1 and TIF2 control energy balance between white and brown adipose tissues. *Cell* **2002**, *111*, 931–41.